Topics in Current Chemistry (2025) 383:3
https://doi.org/10.1007/s41061-024-00486-5

REVIEW

Hybrid Metal-Organic Frameworks (MOFs) for Various Catalysis Applications

Virender Virender[1] · Vandana Pandey[2] · Gurjaspreet Singh[3] · Pawan Kumar Sharma[4] · Pankaj Bhatia[2] · Alexander A. Solovev[5] · Brij Mohan[6]

Received: 22 May 2024 / Accepted: 22 November 2024 / Published online: 13 December 2024

Abstract

Porous materials have been gaining popularity in catalysis applications, solving the current ecological challenges. Metal-organic frameworks (MOFs) are especially noteworthy for their high surface areas and customizable chemistry, giving them a wide range of potential applications in catalysis remediation. The review study delves into the various applications of MOFs in catalysis and provides a comprehensive summary. This review thoroughly explores MOF materials, specifically focusing on their diverse catalytic applications, including Lewis catalysis, oxidation, reduction, photocatalysis, and electrocatalysis. Also, this study emphasizes the significance of high-performance MOF materials, which possess adjustable properties and exceptional features, as a novel approach to tackling technological challenges across multiple sectors. MOFs make it an ideal candidate for catalytic reactions, as it enables efficient conversion rates and selectivity. Furthermore, the tunable properties of MOF make it possible to tailor its structure to suit specific catalytic requirements. This feature improves performance and reduces costs associated with traditional catalysts. In conclusion, MOF materials have revolutionized the field of catalysis and offer immense potential in solving various technological challenges across different industries.

Extended author information available on the last page of the article

Graphical Abstract

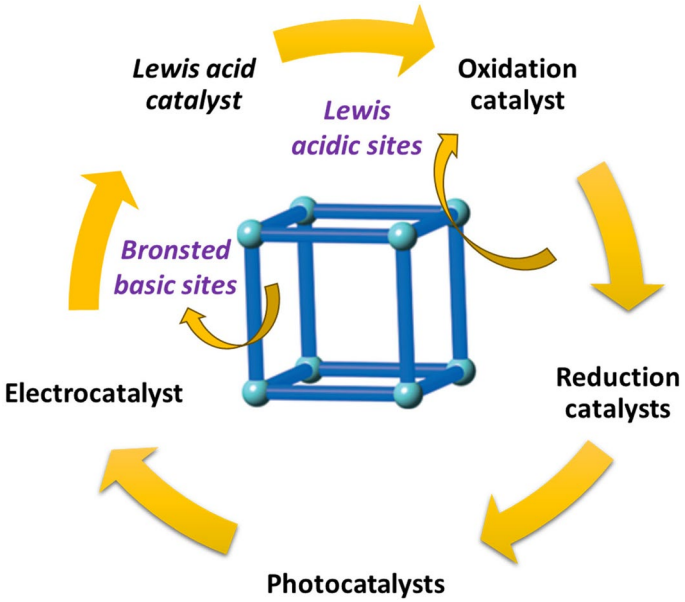

Keywords Metal-organic frameworks · Functionalities · Catalysis · Photocatalysis · Electrocatalysis

1 Introduction

Porous materials refer to substances that have interconnected voids or pores within their structure [1–3]. Depending on the material and intended use, these voids range in size and shape. Porous materials are commonly used in various applications, such as filtration, insulation, catalysis, and drug delivery [4, 5]. The porosity of these materials allows them to absorb and retain liquids or gases, making them useful in many industries [6]. Some examples of porous materials include activated carbon, zeolites, metal-organic frameworks (MOFs), and aerogels. Hybrid metal-organic frameworks (MOFs) have attracted considerable attention recently because of their potential use in numerous catalytic processes [7–9]. These materials are composed of both organic and inorganic components, giving them unique properties that can be tailored for specific chemical reactions. MOFs have shown promising results in areas such as gas storage, drug delivery, and sensing, and their use in catalysis is fascinating [10, 11]. By incorporating various metals into the framework structure, MOFs can serve as efficient catalysts for different reactions, including oxidation, hydrogenation, and even carbon dioxide conversion [12, 13]. The versatility of hybrid MOFs makes them an attractive option for researchers looking to develop new and innovative catalytic processes.

The MOF family of porous materials, often called porous coordination polymers (PCPs), are constructed by connecting inorganic nodes with organic ligands [14]. This unique integration provides MOFs with superior physicochemical properties, leading to substantial research interest worldwide [15]. MOFs are highly porous structures with remarkable properties, including significant surface area, tunable pore size, and exceptional stability, allowing their wide-scale applicability in environment and energy-related domains [7]. MOFs have demonstrated significant potential as highly effective catalysts for various activities by offering active surface sites enabling chemical processes with enhanced efficiency [16]. The size and diameter of the pores in the MOFs are determined mainly by the length of the organic ligands and the numerous interactions they set up with the metallic centers. This, in turn, considerably affects the catalytic activity. However, the effective immobilization of molecular catalysts in MOFs is attributed to the specific surface area and volume of the pores that result from these ligands within the network.

The importance of MOF's active sites from metal and acid/base sites on organic linkers in catalytic applications is highly appreciable [17]. However, the limited options for active sites significantly limit their applications. Still, MOF fabrications allow for the expansion of the source of active sites through pre-introduction or post-synthesis engineering of metal clusters and organic linkers [18]. Additionally, MOFs' inherent ability to enclose various catalytically active species within their pores further promotes efficient catalytic reactions. Moreover, functionalized MOFs substantially facilitate catalytic applications owing to the expansive specific surface sites, remarkable stability, and adjustable structural features [19, 20]. MOF fabrication and production involve creating highly porous materials with various applications. MOFs are particularly useful in treating wastewater contaminated with metal ions, offering an efficient and sustainable solution for environmental remediation [21]. For example, MOFs can selectively adsorb heavy metal ions such as lead, cadmium, and mercury from industrial wastewater, ensuring cleaner water resources and preventing harmful pollutants from entering the ecosystem [22]. Moreover, MOFs can potentially address the growing concern about plastic waste, including PET plastics. Using MOFs in the recycling process, PET plastics can be broken down and transformed into valuable products, reducing the environmental impact of plastic pollution [23]. This innovative approach promotes recycling and waste management and contributes to the circular economy by converting waste materials into new resources.

Some applications of these materials include their use as adsorbents in aqueous solutions, owing to their unique properties, structural characteristics, and affordability [24]. Researchers have recently begun using computational screening to discover adsorbent materials from databases. This approach is practical because of faster computers and improved synthesis of MOFs, enabling targeted design of MOFs with high success rates [25]. Moreover, the rise of machine learning and big data has enabled more efficient searching of MOF chemical space. High-throughput computational screening can offer insights into structure-function relationships. A high-throughput DFT workflow created the Quantum MOF Database, providing quantum-chemical properties for thousands of MOFs. However, the PBE exchange-correlation function can lead to errors in predicting electronic properties, especially

band gaps. Methods to improve machine learning-predicted band gaps for inorganic solids include training models on experimental data and conducting higher-accuracy DFT calculations [26, 27]. Novel studies and approaches have been developed to utilize new forms of energy derived from renewable sources. One such development is using MOFs as electrochemical capacitors and fuel electrodes for rechargeable batteries [28, 29]. Moreover, post-synthetic techniques can modify the structure and porosity of MOFs, making the material more selective and more effective in the CO_2 adsorption process [30, 31]; these modifications result in an efficient catalytic process [32]. MOFs have played a crucial role in heterogeneous catalysis due to their significant physical and chemical properties. Recent studies have demonstrated that novel materials that exhibit properties similar to the parent MOF and the added material can be developed by hybridizing external components with pre-existing MOFs; these are used in many applications, such as drug delivery, catalysis, detoxification, gas storage and separation, energy storage, sensing and lighting, proton conductivity, and supercapacitors [33–38].

MOF hybrid materials have proven to be more effective than their parent materials. Hybrid MOFs are advanced materials that consist of metal ions or clusters linked by organic molecules, resulting in a highly organized, porous crystalline structure. The metal nodes usually consist of transition metals, which provide structural integrity and coordination sites [39]. Organic linkers, often featuring functional groups, connect the metal centers and define the framework's topology and porosity. This specific combination allows for a wide array of arrangements, resulting in MOFs with specific pore sizes and chemical functionalities that can be tailored for various applications. The versatile nature of hybrid MOFs results in numerous practical applications, particularly in gas storage, separation, and catalysis [40]. Their large surface area and adjustable pore sizes make them exceptional candidates for capturing gases such as carbon dioxide or hydrogen, supporting energy storage and environmental remediation efforts. The functionalization of organic linkers enables selective adsorption and chemical reactions, thus enhancing their function in catalysis and drug delivery systems. As research in this field advances, hybrid MOFs consistently demonstrate potential for new applications across diverse industries, from renewable energy technologies to pharmaceuticals [15]. In catalysis, hybrid MOFs can provide active sites for chemical reactions, facilitating oxidation, reduction, and organic synthesis processes, thus contributing to greener chemical manufacturing methods.

Materials such as metals, metal oxides, nanomaterials, covalent-organic frameworks, carbon tubes, rods, enzymes, and acids have been designed as catalysts [41, 42]. Each material has its unique properties for specific reactions. For example, platinum is commonly used as a catalyst in catalytic converters to reduce harmful vehicle emissions [43]. Enzymes are often used in the food industry to speed up reactions and improve product quality. The choice of catalyst depends on factors such as reaction conditions, reaction rate, and selectivity. By carefully selecting the appropriate catalyst, industries can improve efficiency and reduce costs while minimizing environmental impact. MOF catalysis is an important emerging approach that has recently gained significant attention [44, 45]. MOF catalysis is particularly necessary when specific reactions are too slow to be practical and require intervention

to expedite the process. MOF catalysis provides an efficient and effective means of accelerating reactions and achieving desired outcomes in various settings, including industrial applications and scientific research [46]. Furthermore, ongoing research into hybrid MOFs is uncovering new functionalities and improving their performance across different applications. Advances in synthesis techniques and computational modeling are enabling the design of MOFs with specific characteristics tailored for targeted uses. Therefore, hybrid MOFs are becoming increasingly important in addressing global challenges, such as energy storage, environmental remediation, and drug delivery [47]. Their adaptability and multifunctionality position them as a promising class of materials in the quest for sustainable solutions and innovative technologies. Without this indispensable tool, our ability to achieve goals would be significantly hindered as we could not do so as efficiently or effectively.

Recently, there has been a lack of comprehensive reviews focusing on the catalytic applications of MOFs [48–51]. Most of these reviews are limited in scope, typically addressing a singular catalytic process without offering a thorough analysis. This review delves deeply into MOF materials, specifically concentrating on their diverse catalytic applications ranging from oxidation, reduction, Lewis's catalyst, and photocatalysis to electrocatalysis. It accentuates the specificity and novelty inherent in these materials while examining their advantages and limitations. The insightful discourse presented within this review distinguishes it as an exemplary contribution to the field, offering invaluable insights to researchers and practitioners. This exploration delves into the potential of MOFs in emerging catalytic applications, serving as a prospectus to investigate the scalability and commercial viability of MOFs for industrial use in catalytic processes aimed at reducing environmental issues.

2 MOF Material Design

Metal, organic ligands, and carbon-based materials are required to create primary MOF material for catalysis applications [52]. These materials have been made with porous and compatible composite materials based on metal, carbon, and biomolecules [7, 53]. Various multidimensional materials have been used for MOF fabrication. The structural design of MOFs involves using organic molecules called ligands, which coordinate with metal ions to form the framework. These ligands can be chosen based on their size, shape, and chemical functionality to tailor the properties of the MOFs [54]. Additionally, linkers are used to connect the metal ions and create a three-dimensional network of the MOFs. Linkers can vary in length and composition, affecting the MOF's stability and porosity [55]. Therefore, carefully selecting ligands and linkers is crucial in designing MOFs with desired properties for specific applications.

MOFs can be prepared using various methods (Fig. 1), including slow evaporation, solvothermal reactions, microwave-assisted synthesis, electrochemical synthesis, mechanochemical synthesis, and sonochemistry [56–58]. Slow evaporation is a simple method that takes longer but can be done at room temperature [59]. Solvothermal reactions use high-pressure vessels and organic solvents to create unique

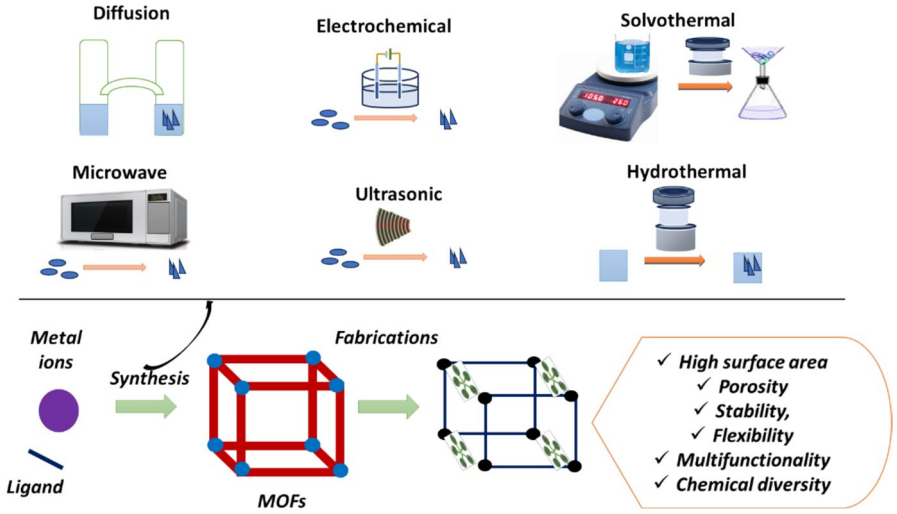

Fig. 1 General MOF synthesis and fabrication for developing composite platforms

morphologies. Microwave-assisted synthesis is fast and involves heating a solution with microwaves for about an hour [60]. Electrochemical synthesis offers continuous production without metal salts. Mechanochemical synthesis uses mechanical force to create chemical reactions without solvents. Sonochemistry uses ultrasound to speed up crystallization time [61].

Among these common synthesis techniques, solvothermal synthesis involves dissolving metal salts and organic ligands in a solvent at elevated temperatures, allowing for better crystallization. This method usually yields high-quality crystals but may be time-consuming and require precise temperature control. However, hydrothermal synthesis uses water as the solvent, enhancing the solubility of certain precursors [62, 63]. It often yields larger crystals with greater porosity but may lead to the formation of less stable frameworks due to the reaction conditions. Microwave-assisted synthesis is popular for its quick and even heating, resulting in shorter reaction times and potentially lower energy usage. However, it may lead to defects if not carefully optimized. Electrochemical synthesis offers precise control over MOF growth but requires specialized equipment and may not be suitable for all frameworks. The choice of synthesis method for MOFs depends on the application and desired characteristics, balancing factors like cost, time, and scalability against the quality and functionality of the final product. It is essential to tailor the synthesis approach to the specific requirements of the intended application. Furthermore, some organic solvents can break down or hydrolyze into other compounds when exposed to high temperatures [64]. Over the past decade, various novel solvent systems have synthesized crystalline MOFs, including ionic liquids, deep eutectic solvents, and surfactants. All these factors can lead to health and environmental concerns. To create new MOFs, it is crucial to use different reaction media that have low vapor pressure and are non-toxic, biodegradable, nonflammable, recyclable, and affordable. Typically, from simulation methods, GCMC is employed to corroborate the equilibrium adsorption isotherms [65], while MD helps investigate the diffusion

of gas molecules within the MOFs. The designed MOFs can also be used to study the effect of different parameters such as temperature, pressure, and pore size to understand and optimize MOF-based applications.

High throughput production of MOFs has been achieved using various techniques, including experimental and computational processes, optimizing synthesis conditions such as temperature, pressure, and time [66]. Adjusting temperature influences crystal growth rate, pressure impacts porosity, and time affects kinetics. Advanced techniques like microwave-assisted synthesis and continuous flow reactors improve speed and scalability. Implementing automated systems for precise control is crucial, and developing screening assays for quick evaluation of MOF properties is important. Combinatorial approaches expedite the exploration of various MOF compositions. This high-throughput synthesis, combined with screening techniques, efficiently navigates the vast landscape of MOF materials [67]. High-throughput predictions of MOFs electronic properties include theoretical challenges, graph neural networks, and data exploration. MOF design attracts interest because of its unique structural features and prospective applications. These porous three-dimensional (3D) structures involving metal ions or clusters linked by organic ligands can be altered and fine-tuned by adjusting the linkers used in their construction. By modifying these organic connectors' chemical structure and composition, researchers can manipulate various aspects of MOF behavior, such as surface area, thermal stability, pore size, and gas adsorption capacity. This level of control over MOF properties opens up exciting possibilities for designing tailored materials with specific functions and characteristics for use in various fields such as catalysis, sensing, separation, and energy storage [68–70].

MOFs' important aspect is their morphology, which refers to the shape and structure of the material. MOFs have many morphologies, including cubes, spheres, rods, and more complex shapes [71, 72]. MOFs' dimensions vary widely, from nanoscale structures to larger particles. Tailoring catalysis requires MOF shape and dimension control. Understanding the variables that affect the morphology and dimensions of MOFs has enabled the development of advanced tools in this field, and it has allowed the development of MOFs as composites of novel materials with improved functionality and performance.

MOFs are designed for catalysis applications because of the exceptional features such as (1) presenting coordination sites on the metal nodes, (2) catalytic sites being found on the linkers, (3) the incorporation of defects, and (4) encapsulating additional catalytic sites such as enzymes, organometallic molecules, and metal nanoparticles to produce multifunctional sites [45, 52, 73]. However, critical points such as instability, lack of coordination between nodes and linkers, and risk to moisture are still certain factors that limit their application in catalysis.

3 MOFs as Catalysts

MOFs' promising applications in heterogeneous catalysis include biomass conversion into biofuels and synthesizing value-added chemicals. Additionally, integrating metal nanoparticles into MOFs can enhance their catalytic performance by

providing additional active sites and improving mass transport. As research in this field advances, more innovative uses for MOF-based catalysts in various industrial processes are developing and fetching researchers' interest [16, 74]. However, when incorporated with other compounds, the resultant materials formed from MOFs exhibit a significantly more durable structure, tunable porosity, and expanded surface area, which are crucial for an appropriate catalyst. Loaded with the above unique characteristics, numerous MOFs such as MOF-74, ZIF-8, CPO-27, UiO-66, CuBDC (HKUST-1), MIL-53, and MIL-101 have been most thoroughly studied as catalytic MOF structures during the past decade [44, 75–77].

3.1 Lewis Acid Catalyst

MOFs act as Lewis acids that can accept an electron pair from another species. MOFs possessing the features of Lewis acids can significantly promote chemical reactions in catalysis by activating reactant molecules and stabilizing transition states [78]. MOFs are effective Lewis acid catalysts for distinct reactions, such as the Diels-Alder and Friedel-Crafts reactions. By tailoring MOFs' metal center and ligand structure, it is feasible to fine-tune their catalytic properties for specific applications. Overall, MOF-based Lewis acid catalysts offer great potential in sustainable chemistry for developing efficient and environmentally friendly processes. For instance, de Vos and coworkers described the catalytic cross-aldol reaction between heptanal and benzaldehyde employing a bifunctional acid–base MOF, UiO-66(NH_2), possessing a $Zr_6O_4(OH)_4$ cluster with an amine group-containing ligand. Notably, Zr(IV) acted as a Lewis acid site, while amino groups served as basic functional groups that promoted/facilitated [79].

Besides, NH_2-MIL-101(Al) MOFs with Lewis acid (Al(III)) and Lewis base (amino group) sites may catalyze tandem Meinwald rearrangement-Knoevenagel condensation (Fig. 2). NH_2-MIL-101(Al) is a strong crystalline material made with amino ligands and Al^{3+} clusters. The amino groups act as bases, and the Al^{3+} centers act as catalysts. The material can be used for Knoevenagel condensation and tandem transformations [80]. Horiuchi et al. described a Knoevenagel condensation reaction, including the catalytic effect of the same MOF on catalyzing deacetalization. The first step involves deacetalization of benzaldehyde dimethyl acetal, facilitated by a Lewis acid Al^{3+} center. The second step, known as the Knoevenagel reaction, is catalyzed by a Lewis base amino group [81].

The synthesis of benzylidene malononitrile and the Knoevenagel condensation of benzaldehyde and malanonitrile were carried out cost-effectively employing a hybrid structure produced using Zn-MOF with a melamine and terephthaldehyde-based covalent organic framework (COF). The proposed catalyst exhibited superior reaction time and performance under specific conditions compared to the previously described catalyst (we need to be specific about the superior outputs) [82]. In an interesting work, Tu et al. demonstrated that the FDM-3–7 (FDM = Fudan material), which is mesoporous and has trinuclear Cu-based pyrazolates coupled with Zn-based units, functioned as a catalyst for the deprotonation of H_2O_2 as well as

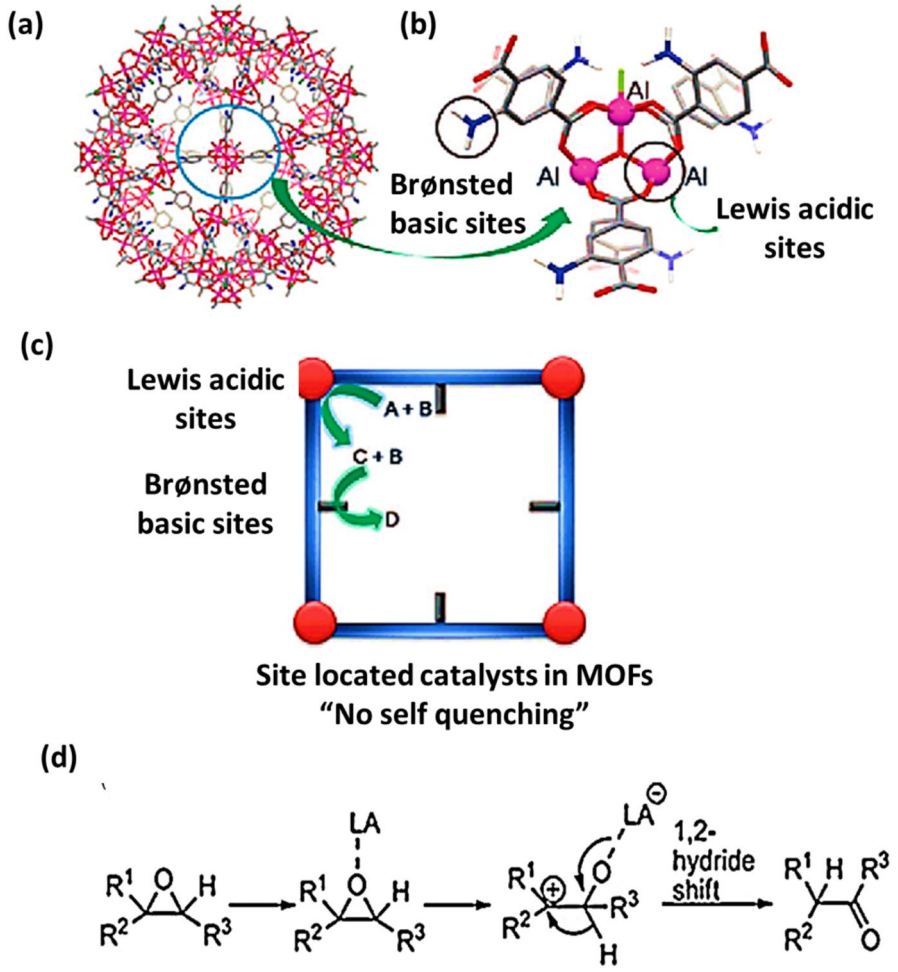

Fig. 2 **a** Large NH_2-MIL-101(Al) cage; **b** the Lewis acidic sites refer to the Al^{3+} centers, while the Brønsted basic sites are represented by the amino terephthalate linkers; **c** a schematic illustration of tandem organic reactions with a site-isolated heterogeneous catalyst; **d** the mechanism of the Meinwald rearrangement entails using a Lewis acid as a catalyst. Reproduced with permission from [80] ©2024 Copyright Clearance Center, Inc. All rights reserved

the oxidation of CO and benzyl alcohol (Fig. 3). The catalytic activity of Cu-based pyrazolates is attributed to the reversible redox reaction of trinuclear Cu sites [83].

$Cu_3(BTC)_2$ (BTC: 1,3,5-benzene tricarboxylic acid) is one of the widely researched, highly selective Lewis acid catalysts. Its application includes applying it as a reusable catalyst in the Fridel-Craft alkylation of indole with β-nitrostyrene [84], the reaction between silanes and pinacolboranes that produces borosiloxanes [85], and the Friedlander reaction, which is involved in the production of tacrine analogs [86]. Han et al. [87] described using MIL-100(Fe) as a highly concentrated Lewis acid catalyst with several Lewis centers for the acetalization of benzaldehyde

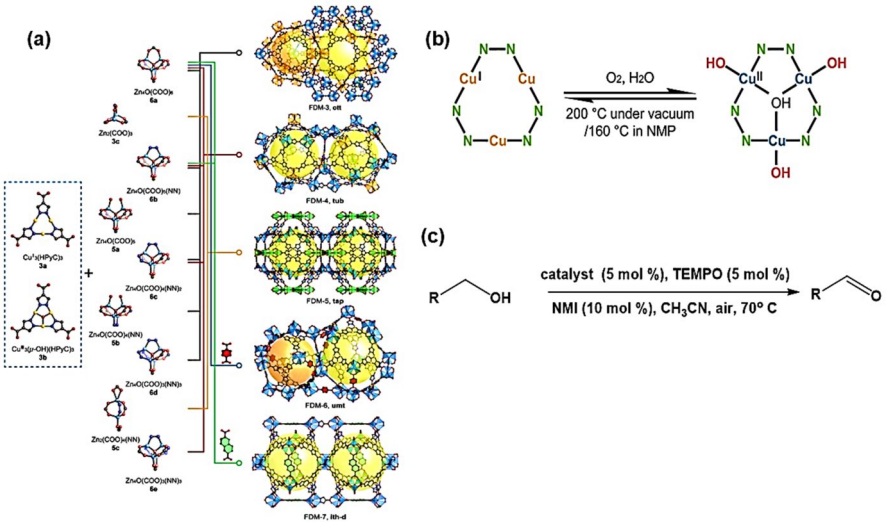

Fig. 3 **a** Multicomponent FDM-3-7 employs SBUs with different geometries using triangular $Cu^{I}_3(HPyC)_3$ (3a) or $Cu^{II}_3(\mu\text{-}OH)(HPyC)_3$ (3b), $Zn_2(COO)_3$ (3c), square-pyramidal $Zn_4O(COO)_4R$ (5a, 5b), trigonal-bipyramidal $Zn_2(COO)_4(NN)$ (5c), and octahedral $Zn_4O(COO)_3R_3$ (6a–6e); five multicomponent MOFs with different topologies were synthesized. Mesopores in FDM-3-7 are shown as yellow and orange spheres. R = COO or NN. **b** Interchangeability of Cu valences in the frameworks of FDM-3-7. **c** Aerobic oxidation of benzyl alcohol and TMBA using FDM-3-7. Reproduced with permission from [83] Copyright ©2017, American Chemical Society

with methanol. Wang et al. achieved 100% ozone conversion efficiency for over 100 h at 45% relative humidity using the same catalyst. Furthermore, it catalyzed the conversion of fructose into lactic acid [88, 89]. Hou et al. developed a MOF with a honeycomb structure, namely BDPO, which refers to N, N′-bis (isophthalic acid)-oxalamide, also known as H_4BDPO. The MOFs possess unsaturated metal sites such as Lewis acids and basic oxalamide groups. This MOF exhibits excellent adsorption selectivity for C_2H_6, C_2H_4, and CO_2 over CH_4, owing to its diverse active sites. The catalyst can be reused, enhancing its practical applications [90].

MOFs are used as nanocatalysts to convert CO_2 into various chemical products, including methane, methanol, ethanol, olefins, heterocycles, and oligomers. Due to their unique features, such as tunable porosity, uniform structure, and greater internal surface area, these materials are known for accelerating reactions of great importance [91]. The synthesis of a 2D tetragonal MOF with high porosity and flexibility was achieved using Zn metal, $Zn(NO_3)_2{\cdot}6H_2O$, and two large size linkers, 1,3,5-tri(1H-benzo[d]imidazol-1-yl)benzene (TBIB) and 1,3,5-tris(4′-carboxyphenyl-)benzene (H_3BTB), under hydrothermal conditions. The resulting MOF is denoted as $([Zn_2(TBIB)_2(HBTB)_2]$ 9DMF $19H_2O)_n$. It catalyzes with various characteristics for the chemical conversion of CO_2 into cyclic carbonates and the production of quinoline derivatives using the Friedländer reaction [92]. Farha et al. successfully synthesized four isostructural mesoporous MOFs, specifically M-NU-1008, using a combination of transition metals (Zr and Hf), lanthanide (Ce), and actinide (Th) [93]. The hexanuclear metal cluster nodes present in these MOFs function

as Lewis acidic sites, facilitating the fixation of CO_2. The facilitated dissociation of water molecules is ascribed to the enhanced catalytic capability of the metal nodes. Among these four, Ce_6-based MOFs demonstrated great potential as Lewis acid catalysts for CO_2 cycloaddition reactions. Copper and calcium-based MOFs were utilized by Koja et al. as catalysts in the esterification and trans-esterification processes to produce biodiesel from waste cooking oil (WCO) [94]. Rai et al. reported the synthesis of a three-dimensional Cu(II)–MOF, $([Cu_2(L)(H_2O)_2]\cdot(3DMF)(4H_2O))_n$, which possesses Lewis acid-base dual functional sites (Fig. 4). The water molecules were removed from the metal centers, allowing the open metal centers to engage in the catalytic conversion of CO_2 into cyclic carbonates under solvent-free conditions [95].

In their study, Guo et al. utilized three different MOF materials—UiO-66, MIL-101, and MOF-5 to investigate the impact of Lewis acid sites on MOFs during the CO esterification process for dimethylcarbonate production. Based on the results, Pd(II)/UiO-66 exhibits superior catalytic activity compared to the other two catalysts. This can be attributed to many Lewis acid sites [96]. In a recent study, Lin et al. demonstrated the effectiveness of a dimension reduction technique in enhancing the accessibility of Lewis acid sites and prolonging the lifetime of a 2D-MOF Zr_6OTf-BTB catalyst. The MOF facilitates sterically hindered multicomponent reactions (MCRs) that result in the production of aziridine carboxylate and tetrahydroquinoline derivatives with high turnover numbers (TONs) [97]. He et al.developed a new Tb-MOF by combining Tb(III) with H_2sbdc (H_2sbdc = 5,5-dioxo-5H-dibenzo [b,d]thiophene-3,7-dicarboxylic acid). It has been demonstrated that the close proximity of the substrate to the Lewis

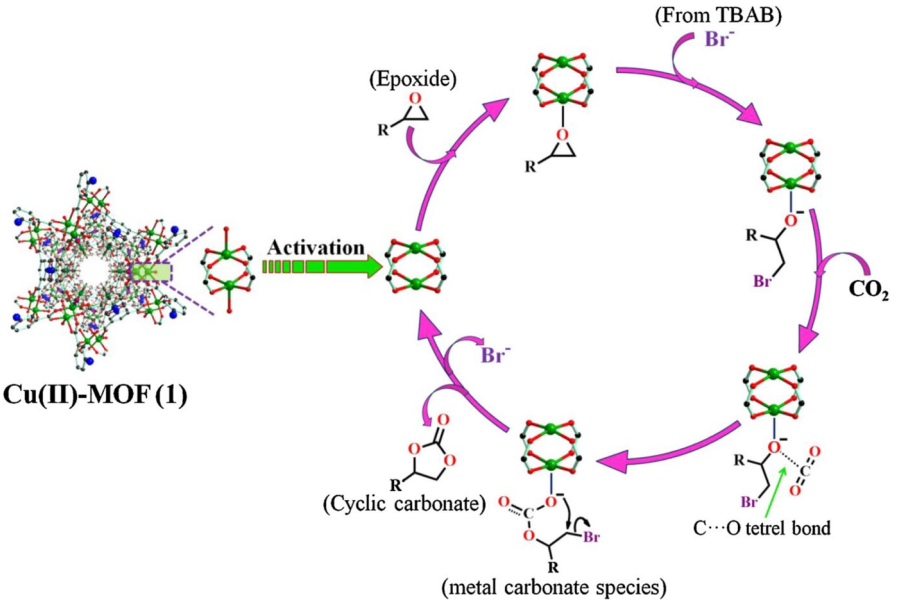

Fig. 4 Proposed mechanism for the chemical fixation of CO_2 catalyzed by Cu-MOF. Reproduced with permission from [95] ©2020 Elsevier Ltd. All rights reserved

acid catalytic sites enables (Tb-MOF) to function as a highly efficient heterogeneous catalyst for the cyanosilylation of aromatic aldehydes under solvent-free conditions at room temperature [98]. In an innovative investigation, Jones et al. were pioneers in utilizing MOFs as a catalyst for the Garcia Gonzalez reaction, exploring the potential of different carbohydrates. They developed UiO-66, utilizing trifluoroacetic acid as a modulator. They utilized a range of linkers during the synthesis process. The material was subsequently tested as a catalyst for converting sugars into polyhydroxy and c-glycosyl furan compounds. The research findings showed that UiO-66-NO_2-20 and UiO-66-H-20 were highly effective catalysts for converting sugars into polyhydroxy and C-glycosyl furan [99]. In a study conducted by Mandal et al. [82], the Lewis acidity of Zn-based MOF (Zn-CBS) and its Zn nanostructure were examined for their potential in catalyzing the Knoevenagel condensation reaction, Friedel-Crafts alkylation, and Strecker reaction. They explained that the catalytic activity of Zn-CBS is attributed to its bifunctional character [100].

An MOF containing Co with exposed Co sites was successfully synthesized and modified to regulate the active centers responsible for catalyzing various CO_2 conversions. Careful control of the active centers has achieved a significant 2.4-fold increase in oxazolidinone yield [101]. A recent report by Maurin et al. discussed a novel MOF known as MFM-300(Sc). This particular MOF has open metal sites that are not permanent and display catalytic properties. Through the Strecker hydrocyanation reaction, the successful demonstration of the reaction between N-benzylideneaniline and TMSCN resulted in the formation of 2-phenyl-2-(phenylamino)acetonitrile. Utilizing the switchable metal sites found on the MOF can facilitate this reaction [102]. In recent research, Zhao et al. [85] explored the catalytic properties of Zn-ZrMOF for detecting profenofos in vegetables, finding it comparable to organophosphorus hydrolase. Based on the study, the Zn-ZrMOF catalyst has Lewis acid-base sites that can break the P-O bond of profenofos [103].

The unique structural features of MOFs allow for accommodating reactant molecules within their pores, facilitating efficient catalysis. Furthermore, modifying the organic ligands and metal nodes in MOFs enables designing catalysts with tailored properties for specific reactions. In addition to their catalytic applications, MOFs have shown promise in environmental remediation and gas separation processes. By leveraging their Lewis acid properties, MOFs can selectively adsorb and remove pollutants from water or separate gas mixtures based on molecular size and affinity. This versatility underscores the significance of MOFs as Lewis acid catalysts in advancing various technological and scientific endeavors. The utilization of MOFs as Lewis acid catalysts represents a burgeoning area of research with vast potential for innovation and advancement. With their customizable structures and exceptional catalytic performance, MOFs continue to captivate researchers seeking novel catalysis solutions.

3.2 Oxidation Catalyst

MOFs have emerged as an up-and-coming platform for developing oxidation catalysts consisting of linked metal ions or clusters. These catalysts play a vital role in enabling chemical reactions involving electron transfer, which are essential for a

wide range of industrial processes, including producing chemicals and fuels. As versatile inorganic-organic hybrid materials, MOFs can be specifically tailored at the molecular level. In addition to functional organic linkers, certain polyoxometalate (POM) clusters may serve as inorganic linkers for developing targeted MOFs that exhibit unique properties [104]. Using MOFs as catalysts, a wide range of organic and inorganic reactions can be performed more efficiently and selectively, opening up many exciting possibilities [105]. Over the past few years, countless MOF materials have been developed that address a range of oxidation reactions, with a particular focus on alcohol, carbonyl compounds, carbon monoxide, sulfur derivatives [106], and other hazardous pollutant oxidation in the environment [107, 108].

In a recent study, Li et al. [86] demonstrated the synthesis and catalytic properties of Ru_3/CN, which was obtained from $Ru_3(CO)_{12}$-ZIF. This catalyst, Ru_3/CN, exhibits an impressive conversion capacity of 100% and a remarkably high turnover frequency for the oxidation of 2-aminobenzyl alcohol. This can be attributed to uniform Ru_3 clusters, which serve as highly efficient sites for improved performance [109]. In 2020, a team of researchers led by Kim developed a unique type of MOF with specialized ligands. These ligands contain 2,2,6,6-tetramethylpiperidin-1-yl) oxyl (TEMPO) groups, which act as active sites for the oxidation of alcohols to ketones when oxygen is present. The MOF, UiO-67-TEMPO-CS, was analyzed to reveal its structure, which consisted of an UiO-67 core with TEMPO and a pure UiO-67 shell. Their research has revealed that the reactions occur exclusively within the pores of the catalytically active core because of selective permeability and surface deactivation effects [110]. Using bimetal-organic frameworks (Co/Fe biMOFs) as a template, porous cobalt ferrite nanocrystals ($CoFe_2O_4$NC) were successfully synthesized. Bisphenol-A (BPA) is effectively degraded by the mesoporous catalyst with a large specific surface area, which activates the oxidant peroxymonosulfate (PMS). The degradation process accelerates as the original solution pH, catalyst dosage, and PMS dosage increase. The enzyme particulate methane monooxygenase (pMMO) catalyzes the oxidation of CH_4 to CH_3OH [111].

Baek et al. successfully developed and synthesized a catalyst called MOF-808-Bzz-Cu in their study. This was achieved through post-synthesis modifications of MOF-808. These copper-oxygen complexes, known as bis(-oxo) dicopper species, were used to stabilize and bind to biologically important imidazole moieties like l-histidine (His), 4-imidazole acrylic acid (Iza), and 5-benzimidazolecarboxylic acid (Bzz). Under isothermal conditions at 150 °C, the catalyst demonstrates remarkable selectivity in converting methane to methanol [112]. Bhadra et al. explored using MOF-based catalysts to oxidize sulfur and nitrogen in fuels, highlighting their effectiveness in this process. Various MOFs such as Ti, V, Co, Zr, Cr, and Fe ions have shown remarkable effectiveness in catalysing oxidative desulfurization (ODS). Various MOFs, including different types such as pristine, composite, bimetallic, and active species-loaded ones, can potentially be used as precursors for synthesizing highly effective oxidation and dehydrogenation catalysts [113]. Yu et al. employed the MOF template approach to produce several $MnCoO_x$/CN catalysts, varying the molar ratios of Mn/Co. They employed bimetal MOFs [MnCo-BDC-DABCO] as the precursor for this purpose (Fig. 5). The Mn_2CoO_x/CN catalyst exhibited excellent catalytic activity and lowered activation energy in the oxidation

process of formaldehyde (HCHO) to carbon dioxide (CO_2) and water (H_2O) at room temperature [114].

Using Ce-based MOFs, Chen et al. developed bimetallic oxides, CeO_2-CuO and Ce-Cu-Ox. Due to the difference in interaction between Cu and CeO_2 species, they have different defect sites and redox properties [115]. Xiao et al. conducted a study on carbon-supported Cu–Co oxide catalysts (Cu–Co/C) with spinel structure and different Co compositions. They utilized Co-doped Cu-based MOF (($Cu_3(BTC)_2 \cdot 3H_2O$ precursor) as the starting material for their research. Because of its wide specific surface area, a substantial amount of surface chemisorbed active oxygen, and a high ratio of Co^{2+}/Co^{3+}, the catalyst $CuCo_{0.5}$/C material demonstrated good catalytic

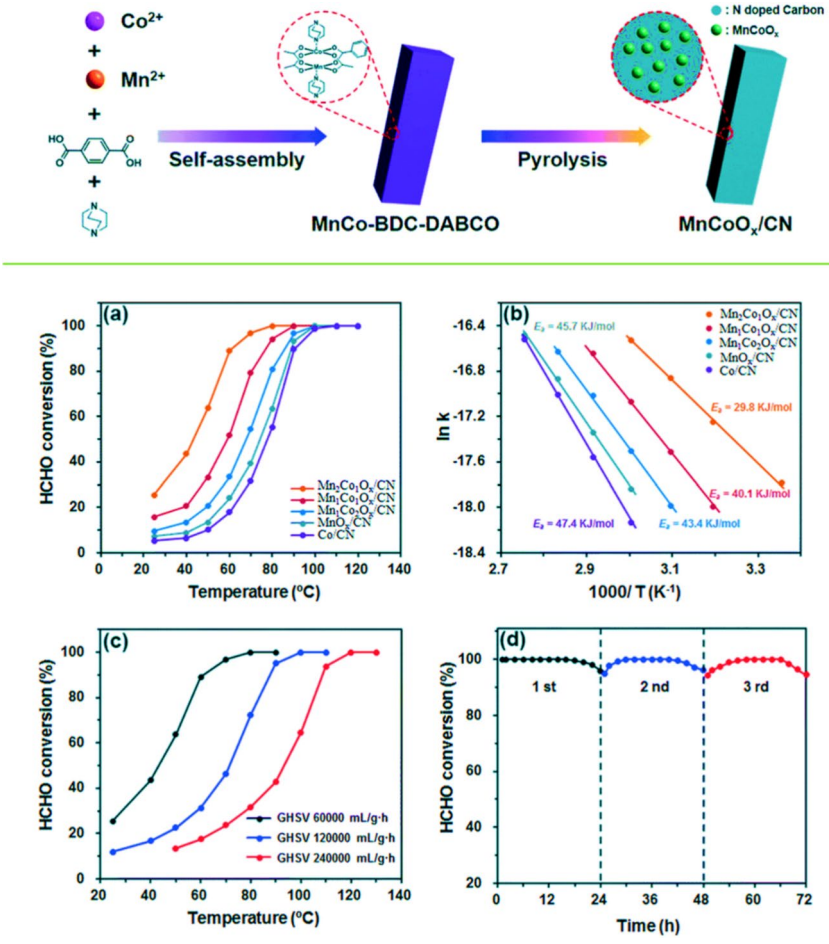

Fig. 5 Illustration of $MnCoO_x$/CN synthesis and **a** catalytic activity HCHO oxidation test, **b** Arrhenius plots for $MnCoO_x$/CN catalysts, **c** influence of space velocity on the catalytic activity of $Mn_2Co_1O_x$/CN, and **d** catalytic stability test of $Mn_2Co_1O_x$/CN. Reproduced with permission from [114]

performance and water resistance in the catalytic oxidation of toluene [116]. Lyu et al. conducted a DFT study to investigate the catalytic efficiency of a mixed metal platform using MIL-100 MOF with various metals (Al, Sc, Ti, V, Cr, Mn, Fe, Co, Ni, Zn, Ru) to oxidize NO to NO_2. According to calculations, the catalytic activity of NO oxidation is enhanced in the Ru(III)/Fe(III) mixed metal MIL-100 [117]. Li et al. have shown the use of Ru@MOFs containing ultra-fine Ru nanoparticles (<2 nm) as the catalyst for aerobic oxidation of monoalcohol and diols to acetal. Ru nanoparticles within the MOF structure facilitate the oxidation of alcohol to aldehyde. The acetalization reaction occurs specifically on the active sites within the MOFs. The catalytic activity and selectivity towards acetals exhibit an ascending trend from Ru@MOF-808(Zr) to Ru@MIL-100(Al) to Ru@MIL101(Cr) [118]. For oxidizing volatile organic compounds, He and coworkers reported on two highly effective MOF-based Co_3O_4 catalysts with different shapes: the spherical Co_3O_4-S, produced from MOF-39, and the rod-like Co_3O_4 (Co_3O_4-R), produced from MOF-74 (Fig. 6). The study demonstrated that the rod-shaped Co_3O_4-R exhibited enhanced catalytic efficiency in the oxidation of o-xylene, with a lower T90% value, higher stability, and enhanced resistance to water compared to the spherical Co_3O_4-S [119].

Keggin hetero polyacid/Ni-MOF composite catalysts (HPW/Ni-MOF, HSiW/Ni-MOF, and HPMo/Ni-MOF) were successfully produced by a one-pot solvothermal method. This involved immobilizing phosphomolybdic acid, tungstophosphoric acid, or silicotungstic acid on Ni-MOF. The catalytic performance was assessed using chemically regulated tests for fatty acid esterification [120]. Several rod-shaped Cu-Mn oxides with multiple interfaces have been developed by the pyrolysis of Cu/Mn-BTC for acetone oxidation. This resulted in the formation of the highly promising HPMo/Ni-MOF stable species. The $CuMn_2O_x$ catalyst demonstrated exceptional catalytic efficiency (T90 = 150 °C), which is attributed to more active oxygen species, defective sites, high water resistance, and long-term stability. It efficiently catalyzes the oxidation of acetone to CO_2 and H_2O, making it a suitable catalyst for removing oxygenated VOCs under high humidity [121]. The catalytic activity of several types of CeO_2/Co_3O_4 mixed nanocomposites, which were developed from

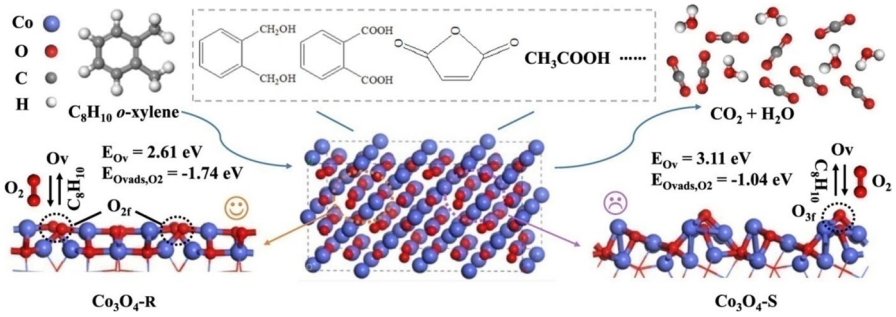

Fig. 6 The catalytic oxidation of *o*-xylene over MOF-based Co_3O_4 with varying shapes, a schematic of the catalytic mechanism. This mechanism demonstrates breaking down the reaction into its components at a spherical or rod-shaped MOF-based Co_3O_4. Produced with permission from [119] Copyright ©2021 American Chemical Society

doping of CeO_2 in parent ZIF-67 base, was evaluated for the oxidation reactions of CO and C_2H_4 [122]. Using the hydrothermal method, Liao and coworkers successfully developed a novel titanium-based MOF material, NH_2-MIL-125. This material demonstrates exceptional desulfurization efficiency when exposed to a temperature of 1500 °C. The DFT analysis revealed the role of hydrogen bonding and π-π stacking in the process. The NH_2-MIL-125@150 °C material exhibits varying adsorption and removal capacities for sulfur-containing compounds (SCCs), following the order of DBT > 4,6-DBT > BT [123]. Salimi and coworkers have published an article on the synthesis of Co-ZIF (ZIF-67) using Co_3O_4 NPs in N-doped porous carbon (Co_3O_4 NPs@N-PC) materials. It is highly effective at catalyzing the antibiotic sulfamethoxazole (SMZ) breakdown. The nano-design demonstrates non-toxic properties, has a high specific surface area, and efficiently activates peroxymonosulfate (PMS) over a wide pH range (2–10) at different temperatures [124]. In their study, Maleki et al. effectively developed bimetallic MOF thin films (UiO-66-sal-Cu$(OH)_2$) using the post-synthesis technique (PSM). This catalyst is designed to efficiently oxidize olefins while being recyclable and environmentally friendly [125].

MOFs have shown great potential in catalyzing the oxidation of organic pollutants in wastewater treatment processes. For instance, MOFs loaded with transition metal ions can effectively degrade organic dyes through oxidation reactions, demonstrating their versatility in environmental remediation applications. The unique properties of MOFs, such as their porosity and large surface area, enable them to adsorb organic molecules and facilitate their oxidation, leading to the removal of harmful contaminants from water sources [126, 127]. In addition to their catalytic applications, MOFs have been explored in other fields, such as gas storage, separation, and sensing. Their ability to adsorb and release gases selectively has made them valuable in storing and separating gases like hydrogen or methane. Furthermore, MOFs integrated with sensing components can detect specific molecules or ions, offering potential uses in environmental monitoring or medical diagnostics.

3.3 Reduction Catalysts

MOFs have become an exciting novel material showing great promise as catalysts for reduction reactions. Thanks to their porous and highly structured network, these materials offer distinct properties that can be utilized in various catalytic applications to facilitate reduction reactions. MOFs are highly efficient in facilitating the removal of oxygen atoms, making them an excellent option for catalysts in reduction reactions. With their exceptional characteristics, MOFs offer a promising option for a wide range of applications in the field of catalysis [128, 129]. Various catalysts incorporating MOFs have been employed to facilitate reduction reactions, such as hydrogenation reactions, involving nitro compounds, aldehydes, imines, and ketones. The synergistic interaction between metal nodes and ligands of MOFs enhances the catalytic performance in hydrogenation.

In a recent study, Qiu et al. reported the synthesis of novel Co@N–C nanocatalysts. These nanocatalysts are synthesized by directly carbonizing a Co-containing MOF structure. The C–N matrix acts as a catalyst for the conversion of

4-nitrophenol to 4-aminophenol in the presence of $NaBH_4$, utilizing Co nanoparticles that are distributed on its surface. This conductive layer facilitates the provision and transportation of electrons for the catalytic reduction reaction [130]. Three Pt@MOF catalysts, including Pt-ZIF-8, Pt-@ZIF-67, and Pt-@UiO-66, were developed using different pore sizes and metal sites. These catalysts were then tested for their ability to selectively hydrogenate two linear unsaturated aldehyde molecules with varied chain lengths. The findings indicate that Pt@ZIF-67, including Co–N clusters, had a greater conversion rate compared to Pt@ZIF-8, which contained Zn–N clusters, in the hydrogenation reaction of the linear unsaturated aldehydes molecule [131]. Farha et al. provided valuable insights into the effect of the MOF microenvironment. They developed eight MOFs using Zr or Hf-based nodes and used them as a platform for depositing one Ni atom per node, forming Ni-M-NU1XXX catalyst species. The catalytic activity of all nickel catalysts supported by Hf-based MOFs is shown to be greater for the hydrogenation of ethylene [132].

The hydrogenation reduction reaction, which involves the conversion of aromatic nitro compounds into aromatic amines, was facilitated by a porous and stable Co–N/C nanocomposite. This composite was developed through the pyrolysis of $Co(2\text{-methylimidazole})_2$ MOF. The catalytic activity is attributed to the high cobalt (Co) concentration, with the dominant form being the highly active β-Co [133]. In their review, Wang et al. thoroughly examined the catalytic capabilities of catalysts based on MOF materials-including N-doped carbon materials, transition-metal phosphides and sulfides, and catalysts based on chemoselective hydrogenation of nitro groups in the presence of one or more reducible groups (C=C, C≡C, C=O, C⁝=N) in this particular application. Selected hydrogenation of the carbon–oxygen group in the presence of the carbon–carbon group is a challenging procedure that converts α,β-unsaturated aldehydes into unsaturated alcohol [134]. Zhao et al. experimented to evaluate the catalytic effectiveness of Pt-based nanostructures, specifically MIL-101@Pt@MIL-101. The nanostructures are composed of Pt nanoparticles sandwiched between a core and a shell composed of MIL-101 (with M being Fe^{3+} or Cr^{3+}). The study demonstrated an evaluation of the efficacy of these nanostructures in converting various types of α,β-unsaturated aldehydes into unsaturated alcohols. The findings revealed that the nanostructures had a notable level of effectiveness and greatly enhanced specificity towards unsaturated alcohols [135]. An ultrathin N-doped graphene nanomesh (NGM) containing highly exposed $Fe\text{-}N_4$ active sites developed from iron phthalocyanine (FePc) exhibits exceptional oxygen reduction reaction (ORR) activity in water (H_2O) [136]. In 2022, a research paper was published by Dhanabalan et al. regarding a hybrid nanostructure composed of Ti-MOF/MoS_2. The researchers revealed that this nanostructure is a durable and recyclable catalyst for converting the hazardous compound 4-nitrophenol (4-NP) in wastewater into 4-aminophenol (4-AP). The reduction reaction occurs in the presence of $NaBH_4$. The process consists of multiple stages, including adsorption, reduction, and desorption. Throughout these steps, the active surface of Ti-OF/MoS2 enables efficient electron transmission. The Ti-MOF/MoS_2 hybrid nanostructure exhibits exceptional catalytic activity in organic reactions, as demonstrated by its ability to efficiently reduce 4-NP to 4-AP using $NaBH_4$ as the reducing agent (Fig. 7) [137].

Recently, Ruan et al. developed an ultrathin bimetallic MOF and used it as a catalyst to reduce 4-NP into 4-aminophenol. The bimetallic Cu-NiMOF showed a quick reduction time of 15 s. This can be attributed to Cu doping, which changes the electron density distribution [138]. Shim and coworkers have synthesized Ce-MOF and Ce-MOF-based CeO_2 catalysts by annealing and investigated their catalytic activity in reducing methylene blue (MB) and rhodamine B (Rh B) in the presence of $NaBH_4$. The latter shows promising catalytic activity compared to the former, with a 90% reduction of the substrate within 8 min [139]. Shen et al. developed a novel catalytic sensing device based on Cu-BTC-MOF to detect gaseous formaldehyde. The catalytic activity of the material is enhanced when it comes into contact with the substrate o-phenylenediamine, which has an NH_2 group. This interaction results in the formation of a colored luminescent compound [140].

MOFs have shown great potential in reducing nitro compounds to primary amines, a key reaction in synthesizing pharmaceuticals and fine chemicals. The unique structure of MOFs allows for precise control over the reaction conditions,

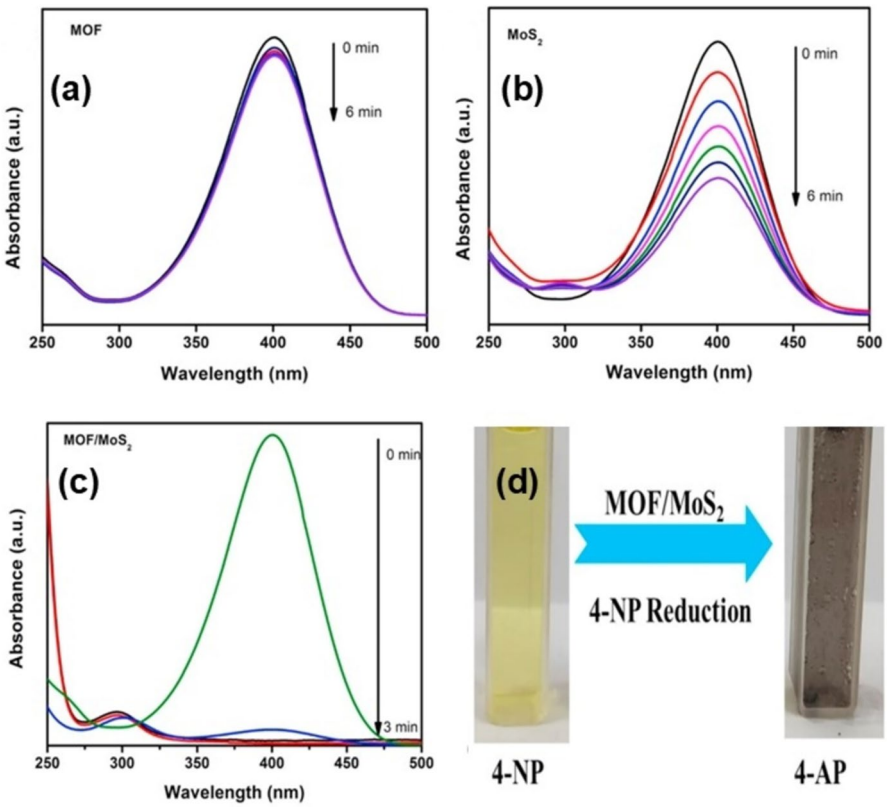

Fig. 7 **a–c** Absorption spectra for conversion of the 4-NP to 4-AP test using MOF, MoS_2, and Ti-MOF/MoS_2. **d** Colorimetric results for conversion of 4-NP to 4-AP using Ti-MOF/MoS_2 catalysts. Reproduced with permission from [137] ©2022 The Authors. Published by Elsevier B.V

leading to enhanced selectivity and yield of the desired products. Additionally, the recyclability of MOF catalysts makes them environmentally friendly and cost-effective alternatives to traditional catalysts. In summary, MOFs exhibit remarkable catalytic performance in reduction reactions due to their structural diversity and tailored functionalities.

3.4 Photocatalysts

MOFs have been proven to be highly efficient photocatalysts in a variety of applications, including water splitting, pollutant degradation, and carbon dioxide reduction [141, 142]. Moreover, the capacity to customize both the composition and structure of MOFs presents ample opportunities for optimizing their catalytic properties and improving their overall performance. MOF-based materials are promising photocatalysts due to the presence of synergistic effects among constituents, their stable nature, and their light absorption capability [143]. Reports suggest the application of MOF-based materials as photocatalysts in several processes, including organic conversions, water splitting, CO_2 reduction, N_2 reduction, and degradation [144, 145]. Trinuclear Mn clusters were used to develop UAEU-50, a manganese-based MOF with a hexagonal layer structure. Its photocatalytic activity was evaluated to determine whether the benzene-dicarboxylate (BDC) linker could catalyze the cycloaddition of different epoxides and CO_2 to produce cyclic carbonates. Its remarkable photocatalytic activities in visible light are attributed to its exceptional chemical and thermal stability. The CO_2 cycloaddition occurs as the UAEU-50's Mn nodes coordinate with oxygen from epoxides, weakening the C-O bond. TBAB triggers the opening of the epoxide ring and activates CO_2 via a photogenerated ligand-to-metal charge-transfer process under light (Fig. 8). The activated CO_2 attacks the C in epoxides, leading to the formation of cyclic carbonates. BDC linker is not a strong visible-light absorption antenna; however, active Mn sites are essential in activating the cycloaddition reaction. Replacing BDC with BDC-NH_2 did not enhance photocatalytic activity [146].

The porphyrin-based metal-organic framework (PMOF) with Fe and Al metals was developed and is also referred to as Al-PMOF-Fe. To ensure stability, the photocatalyst used for the N_2 reduction reaction (NRR) includes Fe as the active center and Al nodes. According to the study, the catalyst's active Fe–N site enhances its ability to adsorb and activate N_2, converting it into NH_3 [147]. The material Fe-MOF (M-300) containing mixed valence Fe sites with Fe^{2+}/Fe^{3+} was produced through thermal treatment of the precursor MIL-100(Fe). It exhibits remarkable efficacy in the degradation of volatile organic compounds and inhibiting the growth of *Escherichia coli* bacteria when exposed to visible light. Also, it is responsible for catalytically degrading acetaldehyde when exposed to sunlight. The presence of exposed unsaturated Fe^{2+} active sites plays a role in transporting photo-generated electrons and reducing O_2 [148]. Weng et al. utilized a simple approach to develop the hierarchically porous HP-UOH-X (HP, UOH, and X representing the hierarchical pores). The material exhibited excellent selective uptake ability for Cr(VI) in various simulated water samples containing competing anions [149]. Lin et al.

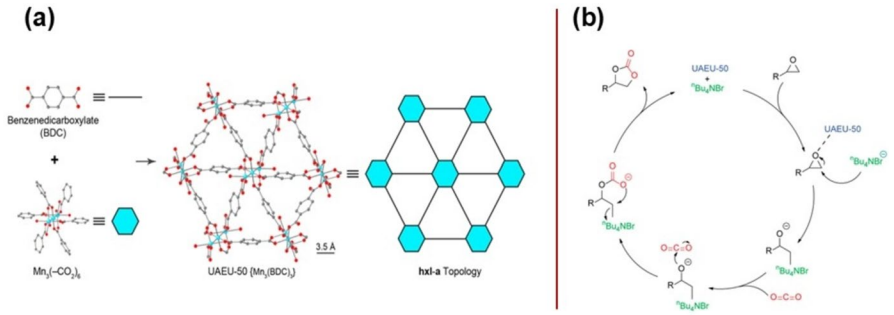

Fig. 8 **a** Trinuclear Mn clusters and benzene dicarboxylate (BDC) combined to generate UAEU-50, which has a 3.5 Å pore size and a hexagonal layer structure. **b** Proposed mechanism of cyclic carbonate formation from epoxides and CO_2. Reproduced with permission from [146] *Copyright* ©2022 The Authors. Published by American Chemical Society

developed two novel titanium-based MOFs, Ti_3-BPDC-Ir and Ti_3BPDC-Ru, by doping Ir/Ru compounds into Ti_3BPDC (BPDC = biphenyl-4,4′-dicarboxylate). These MOFs are photosensitizers in the hydrogen evolution reaction (HER) driven by visible light. The reaction proceeds via the process of reductive quenching of the excited photosensitizer, followed by electron transfer from the reduced photosensitizer to the ($Ti_3(OH)_2$) secondary building unit [150].

By including light sensitization, inserting catalytic sites within MOFs, and modifying the functional group, the use of MOF-based moieties in heterogenous photocatalysis for H_2 production from water can be enhanced [151]. Li et al. developed a highly effective photocatalyst (Pt/def-TiO_2) for hydrogen (H_2) production by assembling single platinum (Pt) atoms on a defective TiO_2 base. The atomic interface between Pt and O-Ti^{3+} facilitates electron transfer, leading to the separation of electron-hole pairs. Therefore, there is improved photocatalytic hydrogen generation with TOF of 51,423 h^{-1}. The Pt1/def-TiO_2 catalyst was used in photocatalytic hydrogen production because of its excellent properties. The def-TiO_2 catalyst performed poorly, but the Pt1/def-TiO_2 catalyst showed significantly enhanced performance with a H_2 production rate of 52,720 µmol g^{-1} h^{-1} (Fig. 9). The Pt NPs/f-TiO_2 catalyst had lower photocatalytic activity with a H_2 production rate of 4458 µmol g^{-1} h^{-1}. The Pt1/def-TiO_2 catalyst achieved record-level photocatalytic H_2 production activity and had an unexpectedly high turnover frequency (TOF) of 51,423 h^{-1} [152]

Lin et al. suggested utilizing unstable Cu^I species in photocatalytic CO_2 hydrogenation to generate ethanol. A new catalyst, $Cu^{II}(HxPO_4)y$@Ru-UiO, was developed by incorporating Cu^{II} species into the photoactive MOF of the UiO-67 structure (Ru-UiO). In the presence of light, [$Ru^{II}(BPY)_2$(BPYDC)]* facilitates the transfer of a lone electron to both Cu^{II} and Cu^0, leading to the formation of CuI. This is crucial for catalyzing the production of ethanol [153]. In their study, Liu et al. discussed the development of a durable and efficient photocatalyst called Ag/AgCl@MIL-88A(Fe) (ACMA). This photocatalyst was developed by combining plasmonic Ag/AgCl with semiconductor-like MOF MIL-88A(Fe) nanocomposites

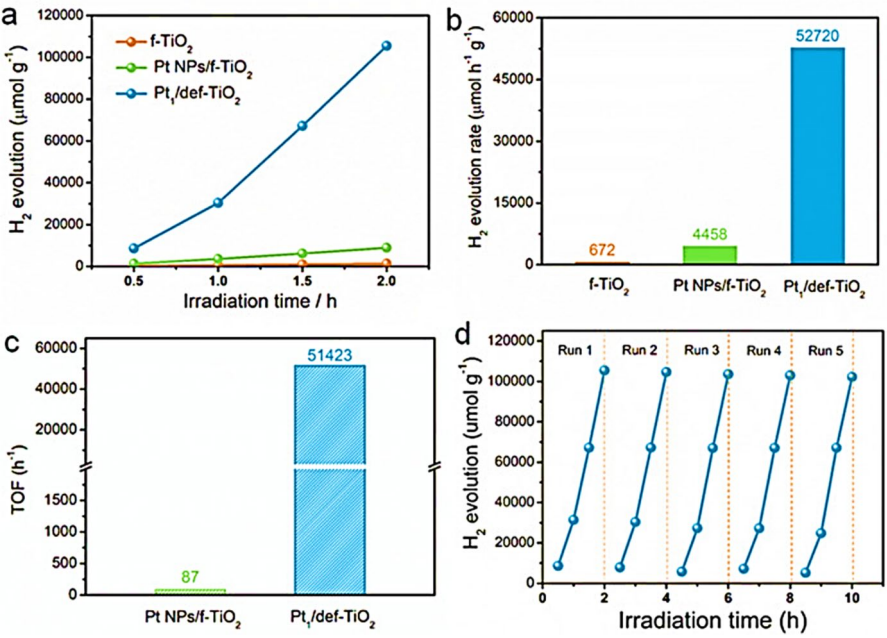

Fig. 9 **a** Demonstration of hydrogen production monitoring over 2 h, with the presence of CH_3OH as sacrificial electron donor. **b** Rate of H_2 evolution. **c** Photocatalytic H_2 production activities. **d** Cyclic tests of Pt_1/def-TiO_2 under UV/Vis light. Reproduced with permission from [152] ©2020 Wiley-VCH Verlag GmbH & Co. KGaA, Weinheim

using the solvothermal approach. This nanocomposite is incredibly efficient at catalyzing the degradation of ibuprofen. The even distribution of Ag/AgCl on the surface of MOF enhances the absorption of visible light and promotes the rate of photoinduced charge transfer [154]. Weng et al. studied the UiO-66-NH_2 (Zr/Hf) membrane as a photocatalyst for reducing Cr(VI) to Cr(III). This membrane showed > 94% efficiency in reducing Cr(VI) after 20 cycles. This high efficiency is due to its exceptional chemical and water stability. The membrane offers a new and effective approach to the photocatalytic removal of pollutants in wastewater [155]. In another report, they used MIL-101(Fe)–NH_2@Al_2O_3 (MA) as a photocatalyst to quickly and effectively reduce Cr(VI) under white light in a laboratory experiment and under real solar light in a field experiment [156].

In photocatalysis, MOFs have shown great potential in driving chemical reactions under light irradiation. One notable example is using MOFs to degrade organic pollutants in water through photocatalytic processes. By harnessing the energy from light, MOFs can activate specific reaction pathways that lead to the degradation of harmful contaminants, thus offering a sustainable solution for water treatment [157]. Moreover, MOFs can be functionalized with different components to enhance their photocatalytic performance. For instance, incorporating photosensitizers or co-catalysts into the MOF structure can improve the efficiency of light absorption and charge separation, leading to enhanced catalytic activity [158, 159]. This ability to

tailor the properties of MOFs makes them versatile materials for a wide range of photocatalytic applications.

3.5 Electrocatalyst

Extensive research has been conducted on the use of MOF materials in the field of clean and sustainable energy storage and electrochemical energy production [160, 161]. The bimetallic catalyst was produced by homogeneously incorporating sub-nanoclusters (CoFe-PPy) onto N-rich nanotube carbon. Through the electrostatic interaction between positively charged N on pyrrole monomers and carboxyl groups on cross-linkers, a remarkable dispersion and supramolecular confinement of Co and Fe species is achieved on PPy backbones. CoFe-PPy exhibits enhanced bifunctional sites, resulting in a high density of active sites and rapid activation of O_2. This material demonstrates enhanced oxygen electrocatalysis for both the oxygen evolution reaction (ORR) and the oxygen reduction reaction (OER) (Fig. 10) [162].

Pyrolysis of MOFs produced the nanostructured stable and recyclable M–N–C catalysts with uniformly distributed active centers, high porosity, and a large surface area. Metal nanoparticles can serve as highly effective electrocatalysts and electrode materials [163, 164]. The electrocatalytic performance of these materials has been thoroughly examined in various reactions, including ORR, OER, and HER, methanol oxidation, reduction of carbon dioxide, sulfur reduction reaction (SRR), and sulfur evolution reaction (SER) [165]. The synthesis of Fe/Ni-based MOFs, Fe_xNi_y-BDC, with low crystallinity was achieved using a solvothermal approach by carefully regulating the reaction between Fe/Ni ions and terephthalic acid (H_2BDC) [166]. The introduction of Ni^{2+} ions led to a mismatch in coordination with organic ligands, resulting in the loss of an organized framework. This caused an increase in defects and a decrease in local crystallinity within the architecture. Using these nanoparticles as an effective catalyst for OER is justified by their low overpotential of 260 mV (at a current density of 10 mA cm^{-2}) and a high

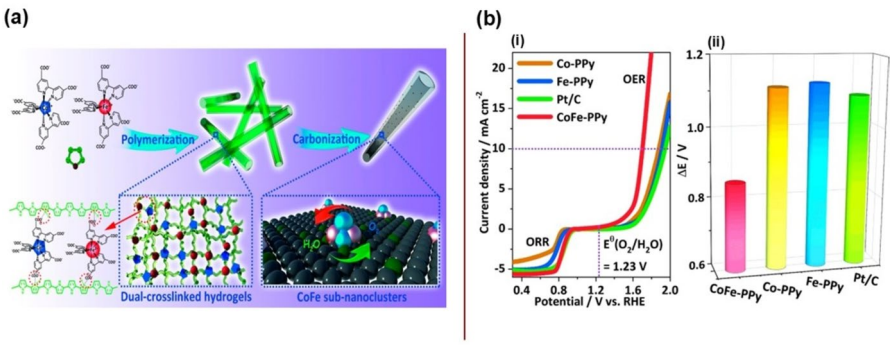

Fig. 10 **a** A graphic illustration of the CoFe-PPy hydrogels synthesis process. **b** Bifunctional activities for oxygen electrocatalysis [(i) = LSV curves collected with an RDE (1600 rpm) at 10 mV s^{-1}; (ii) = the bar diagram of the potential difference (ΔE) between $EJ10$ for OER and $E_{1/2}$ for ORR]. Reproduced with permission from [162] Copyright ©2019 American Chemical Society

turnover frequency of 0.36 s^{-1} at 330 mV in an alkaline solution. A highly effective and reliable electrocatalyst for OER is produced by using crystalline silver (Ag) and amorphous nickel–cobalt–molybdenum oxides (NCMO) on a nickel foam (NF). The findings demonstrate that modification of the electronic structure at the interfacial regions reduces the overpotential for OER [167]. Meng et al. recently synthesized an amorphous-crystalline (AC) heterostructure MS/$Ni_{0.6}$7$Fe_{0.33}$-MOF by incorporating metal sulfide into $Ni_{0.67}Fe_{0.33}$-MOF. It is a durable and stable electrocatalyst for water-splitting systems [168]. Xu et al. proposed a stable electrocatalyst, RuO_2@CNT@MOF, composed of ruthenium dioxide-doped carbon nanotubes and a bismuth metal porphyrin-based MOF. This catalyst demonstrates excellent performance in HER, as evidenced by its low overpotential in both acidic (50 mV) and alkaline (13 mV) media. The enhanced absorption of hydrogen ions and the formation of hydroxyl ions can be attributed to the highly symmetrical conjugated structure of the Bi-porphyrin MOF. RuO_2@CNT@MOF was tested for electrocatalytic activity in HER using a three-electrode configuration (Fig. 11). The performance of the catalyst was compared to other reference samples, including CNT, Bi-TCPP MOF, and commercially available RuO_2. Results showed that RuO_2@CNT@MOF required only 13 mV to reach a current density of 10 mA cm^{-2} and achieved commercial Pt/C catalytic activity [169].

Srivastava et al. reported three simple nickel-based bifunctional electrocatalysts capable of HER and OER activity in alkaline and acidic medium. The stable core-shell Ni@NCS nanomaterials, specifically Ni@NCS-600, Ni@NCS-700,

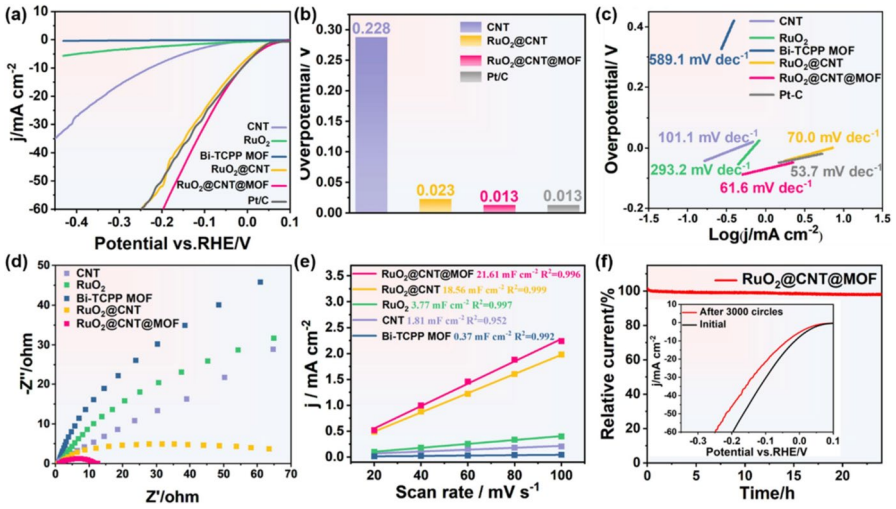

Fig. 11 **a** Comparison of HER polarization curves for CNT, RuO_2, Bi-TCPP MOF, RuO_2@CNT, and RuO_2@CNT@MOF with Pt/C. **b** Overpotential comparison of different electrodes at current densities of 10 mA/cm^2. **c** Tafel slopes for different samples. **d** EIS spectra of CNT, RuO_2, Bi-TCPP MOF, RuO_2@CNT, and RuO_2@CNT@MOF. **e** C_{dl} values of CNT, RuO_2, Bi-TCPP MOF, RuO_2@CNT, and RuO_2@CNT@MOF. **f** Chronoamperometric measurement of HER at the current density of 10 mA cm^{-2} (inset is polarization curves of RuO_2@CNT@MOF initial and after 3000 CV scans for HER). **a**–**f** In 1 M KOH. Reproduced with permission from [169] ©2022 Elsevier B.V. All rights reserved

and Ni@NCS-800, are produced from the pyrolysis of Ni-MOF. The exceptional dual-functional activity of these electrocatalysts, particularly Ni@NCS-800, is supported by their low overpotential and Tafel slope [170]. Lee et al. successfully developed a nitrogen co-doped carbon framework (CoP-NC@NFP) using a MOF-based approach. This framework consists of a core made of CoP-NC and a shell composed of NFP bi-metallic phosphide (NFP, NiFeP) nanoflakes. The resulting structure has several active sites. The purpose of green technology includes the electrochemical reduction of CO_2 to produce compounds for industrial applications. The CO_2 reduction reaction proceeds through a mechanism that involves the transfer of numerous electrons, resulting in the synthesis of diverse products including carbon monoxide, formic acid/formate, methane, ethylene, acetic acid/acetate, ethanol, and n-propanol [171].

Copper-based catalysts have exhibited exceptional efficacy in the process of CO_2 reduction reaction [172]. Jeong et al. reported the use of Cu-based MOFs, MOF/GO composites based on Cu–benzene-1,3,5-tricarboxylic acid [$Cu_3(BTC)_2$], and graphene oxide, for electrochemical conversion of CO_2 into formic acid. This conversion was carried out using six different supporting electrolytes with a high efficiency of 66.57 mM (− 0.6 V) using a 0.1 M TBAB/DMF electrolyte. A two-dimensional conjugated MOF, PcCu–O_8–Zn, consisting of stacked layers, was designed and synthesized. It includes copper phthalocyanine (CuN_4) as the ligand and zinc-bis(dihydroxy) complex (ZnO_4) as the linkage. This MOF then served as an electrocatalyst for converting CO_2 to CO. The ZnO_4 complexes acted as catalytic sites for CO_2 reduction, while CuN_4 centers facilitated the protonation of adsorbed CO_2 during the CO_2 reduction reaction [173]. Using MOFs in the electrochemical reduction of oxygen is a crucial reaction in fuel cells for energy conversion. The precise control over the composition and structure of MOFs enables designing electrocatalysts with high activity and selectivity. Furthermore, functionalizing MOFs with different groups or dopants further enhances their electrocatalytic performance. By introducing specific functional groups, such as nitrogen-containing ligands, the catalytic activity of MOFs can be tailored to particular reactions. This level of customization is particularly advantageous in designing electrocatalysts for complex reactions with stringent requirements. A summary of MOF-based catalysts for different reactions is given in Table 1.

4 Findings and Challenges

MOFs have also been explored for their potential in gas storage, separation, and sensing applications. Their tunable pore sizes and surface functionalities make them promising candidates for these fields. Additionally, MOFs have shown promise in drug delivery due to their ability to encapsulate and release molecules in a controlled manner. The versatility of MOFs has led to extensive research and development in various industries, including energy, environmental remediation, and biomedical engineering. As new advancements are made in synthesizing and characterizing MOFs, their potential applications continue to expand. To produce multifunctional sites (MFS), a variety of techniques are utilized, including the use of coordination

Table 1 Summary of MOF-based catalysts for different reactions

Reaction	MOFs	Substrate	Type	Refs.
Cross aldol reaction	UiO-66(NH_2)	Heptanal and bezaldehyde	Lewis acid catalyst	[79]
Tandem Meinwald rearrangement Knoevenagel condensation reaction	NH_2-MIL-101(Al)	Epoxide and active methylene compounds	Lewis acid catalyst	[80]
Deacetalization–Knoevenagel condensation	MIL-101(Al)-NH_2	Benzaldehyde dimethylacetal and malononitrile	Lewis acid catalyst	[81]
Knoevenagel condensation	Zn-MOF/COF	Aromatic aldehyde and malononitrile	Lewis acid catalyst	[82]
Oxidation and decomposition	FDM-3-7	CO, benzyl alcohol, H_2O_2	Redox active Cu^{II}/Cu^{I}	[83]
Friedel–Crafts alkylation	$[Cu_3(BTC)_2]$	Indole, β-nitrostyrene	Lewis acid catalyst	[84]
Oxidative hydrolysis coupling	$[Cu_3(BTC)_2]$	Silanes and pinacolboranes	Lewis acid catalyst	[85]
Friedländer reaction	$[Cu_3(BTC)_2]$	5-Amino-4-cyano-2-phenyl-1,3-oxazole and carbonyl derivatives	Lewis acid catalyst	[86]
Acetelization reaction	MIL-100(Fe)	Benzaldehyde with methanol	Lewis acid catalyst	[87]
Ozone conversion	MIL-100(Fe)	Ozone	Lewis acid catalyst	[88]
Transformation reaction	MIL-100(Fe)	Hexose sugar	Lewis acid catalyst	[89]
Adsorption and chemical fixation of CO_2	$([Ba_2(BDPO)(H_2O)]\cdot DMA)_n$	C_2H_6, C_2H_4, and CO_2	Lewis acid catalyst	[90]
Cycloaddition reaction and Friedländer reaction	$([Zn_2(TBIB)_2(HTCPB)_2]\cdot 9DMF\cdot 19H_2O)_n$	CO_2, aromatic 2-aminoketone and active methylene compounds	Lewis acid catalyst	[92]
Cycloaddition	M-NU-1008	CO_2 and styrene oxide	Lewis acid catalyst	[93]
Esterification and transesterification reactions	Cu + Ca-MOF	Waste cooking oil (WCO)	–	[94]
Adsorption and chemical fixation	Cu(II)-MOF	CO_2, epoxides	Lewis acid catalyst	[95]
Esterifiaction	UiO-66, MIL-101 and MOF-5	CO	Lewis acid catalyst	[96]

Table 1 (continued)

Reaction	MOFs	Substrate	Type	Refs.
(a) Diels–Alder reactions (b) Povarov reaction (c) Aziridine carboxylate synthesis	Zr_6OTf-BTB	(a) 1,4-Benzoquinone and cyclohexa-1,3-dien (b) Aniline, aldehyde, and activated olefin (c) Aniline, benzaldehyde, and ethyl diazoacetate	Lewis acid	[97]
Aldehyde cyanosilylation	Tb-MOF	Aromatic aldehye and trimethyl silyl cyanide	Lewis acid	[98]
Gracia–Gonzalez reaction	UiO-66	Aldose and acetyl acetone		[99]
(a) Knoevenagel condensation, (b) Friedel–Crafts alkylation and Strecker reaction	$([Zn_4(\mu_3\text{-}OH)_2(D\text{-}2,4\text{-}cbs)_2(H_2O)_4]\cdot 5H_2O\}_n$ (Zn-CBS) and its nanostructures	(a) Malononitrile and aldehyde (b) aldehyde and indole (c) Acetophenone, aniline, and TMSCN	Lewis acid	[100]
Cycloaddition	$((NH_2Me_2)[Co_3(\mu_3\text{-}OH)(BTB)_2(H_2O)]\cdot 9H_2O\cdot 5DMF)_n$	CO_2 and aziridines	Lewis acid	[101]
Strecker hydrocyanation reaction	MFM-300(Sc)	*N*-Benzylideneaniline and trimethylsilyl cyanide (TMSCN)	Lewis acid	[102]
Organophosphorus hydrolase	Zn-ZrMOF	Profenofos	Lewis acid	[103]
Oxidation reaction	Ru_3/CN from $Ru_3(CO)_{12}$@ZIF-8	2-Aminobenzyl alcohol	Oxidation	[109]
Anerobic oxidation reaction	UiO-67 TEMPO-CS	Alcohol	Oxidation	[110]
Degradation reaction	Co/Fe bi-MOF($CoFe_2O_4$ NC)	Bisphenol	Oxidation	[111]
Oxidation	MOF-808-Bzz-Cu	Methane	Oxidation	[112]
Oxidation	MnCo-BDC-DABCO($Mn_2Co_1O_x$/CN)	Formaldehyde	Oxidation	[114]
Oxidation	Ce-MOF(CeO_2-CuO)	CO	Oxidation	[115]
Oxidation	$Cu_3(BTC)_2\cdot 3H_2O$($CuCo_{0.5}$/C)	Toluene	Oxidation	[116]
Oxidation	MIL-100(Fe), MIL-100(Fe–Mn)	NO	Oxidation	[117]
Oxidation	Ru@MOF-808(M) M = Zr, Al, Cr(	Monoalcohol and diol	Oxidation	[118]
Oxidation	MOF-74 (Co_3O_4-R)	*o*-Xylene		[119]
Esterification	HPMo/Ni-MOF	Fatty acids		[120]

Table 1 (continued)

Reaction	MOFs	Substrate	Type	Refs.
Oxidation	Cu/MnBTC($CuMnO_x$)	Acetone		[121]
Oxidation	ZIF-67(CeO_2/Co_3O_4)	CO and C_2H_4		[122]
Oxidative desulfurization	MOF-808(Ce)-F-H	Dibenzothiophene		[180]
Adsorptive desulfurization	NH_2-MIL-125	DBT,4,6-DBT,BT	Oxidation	[123]
Oxidative degradation	ZIF-67(Co_3O_4 NPs@N-PC)	Sulfamethoxazole	Oxidation	[124]
Epoxidation	UiO-66-Sal-Cu$(OH)_2$	Cyclooctene		[125]
Reduction	ZIF-67(Co@N-C700)	4-Nitrophenol	Reduction	[130]
Hydrogenation	ZIF-67(Pt@ZIF-67)	Citronellal	Reduction	[131]
Hydrogenation	Ni-M-NU-1XXX (M = Zr, Hf)	Ethylene	Reduction	[132]
Hydrogenation	Co(2-methylimidazole)$_2$(Co-N/C)	Aromatic nitro compounds	Reduction	[133]
Hydrogenation	MIL-101@Pt@MIL-101,	α,β-Unsaturated aldehydes	Reduction	[135]
Oxygen reduction	FePc(SA-Fe-NGM)	O_2	Reduction	[136]
Hydrogenation	Ti-MOF/MoS_2	4-Nitrophenol	Reduction	[137]
Hydrogenation	CuNi-MOF	4-Nitrophenol	Reduction	[138]
Hydrogenation	CeMOF/CeO_2	MB and RhB	Reduction	[139]
–	Cu-BTC	*o*-phenylenediamine	Reduction	[140]
Cycloaddition	UAEU-50	CO_2	Photocatalyst	[146]
Reduction	Al-PMOF-Fe	N_2	Photocatalyst	[147]
Reduction	MIL-100 Fe(M-300)	VOCs and acetaldehyde	Photocatalyst	[148]
Adsorption/Desorption	HP-UOH-X	Cr(VI)	Photocatalyst	[149]
Hydrogen evolution	Ti_3BPDC M (M = Ir, Ru)	H_2O	Photocatalyst	[150]
Hydrogenation	$Cu^{II}(H_xPO_4)_y$@Ru-UiO	CO_2		[153]
Degradation	Ag/AgCl@MIL-88A(Fe)	Ibuprofen	Photocatalyst	[154]
Reduction	UiO-66-NH_2(Zr/Hf)	Cr(VI)	Photocatalyst	[155]

Table 1 (continued)

Reaction	MOFs	Substrate	Type	Refs.
Reduction	MIL-101(Fe)–NH_2@Al_2O_3 (MA)	Cr(VI)	Photocatalyst	[156]
OER, ORR	CoFe-PPy		Electrocatalyst	[162]
OER	Fe-BDC(Fe_xNi_y-BDC)	H_2O	Electrocatalyst	[166]
OER	Ag/NCMO/NF	H_2O	Electrocatalyst	[167]
OER	MS/$Ni_{0.67}Fe_{0.33}$-MOF	H_2O	Electrocatalyst	[168]
HER	Bi-TCPP MOF(RuO_2@CNT@MOF)	H_2O	Electrocatalyst	[169]
OER, HER	Ni-MOF(Ni@NCS-800)	H_2O	Electrocatalyst	[170]
OER, HER,ORR	NiFeP(CoP-NC@NFP)	H_2O	Electrocatalyst	[171]
Electro-reduction	$Cu_3(BTC)_2$(Cu-BTC/GO)	CO_2	Electrocatalyst	[172]
Electro-reduction	PcCu-$(OH)_8$(PcCu-O_8-Zn/CNT)	CO_2	Electrocatalyst	[173]

sites on metal nodes, catalytic sites present on linkers, incorporation of defects, and encapsulation of additional catalytic agents such as enzymes, organometallic molecules, and metal nanoparticles. These methods work together to create a highly efficient system that simultaneously performs multiple functions.

MOFs are versatile materials with promising catalytic activity in both alkaline and acidic media, and they are ideal for energy conversion and storage technologies. Specifically, MOFs with cobalt or nickel ions show enhanced catalytic performance in splitting water molecules for hydrogen gas production. Metal selection is crucial for optimal HER activity in MOFs. In the OER, MOFs promote the oxidation of water molecules to produce oxygen gas. Tailoring the composition and morphology of MOFs enhances their electrocatalytic properties for increased OER efficiency [174, 175]. Functional groups or dopants can significantly impact the catalytic behavior of MOFs towards OER. The tunable nature of MOFs allows customization for specific reaction conditions in alkaline or acidic environments. Understanding structure-property relationships in MOFs helps optimize design for improved activity in different media. The coordination sites on metal nodes act as anchor points for the catalytic agents, while the catalytic sites on linkers facilitate the necessary chemical reactions. Incorporating defects into the system allows for enhanced reactivity and selectivity while encapsulating additional catalytic agents, further broadening the range of functions that can be performed.

MOFs offer high catalytic performance and tunable properties for efficient energy conversion processes. MOFs have demonstrated their versatility in various chemical reactions and catalytic processes. As Lewis acid-base catalysts, MOFs have shown exceptional activity in promoting organic transformations by facilitating the formation of new chemical bonds. For example, MOFs have been utilized for synthesizing pharmaceutical compounds to enhance the efficiency of key reactions, leading to higher yields and purities [58, 176]. Moreover, MOFs have also proven effective in oxidation reactions, which can selectively oxidize specific functional groups within a molecule. This selectivity is crucial in the pharmaceutical industry, where precise control of the oxidation state of a compound is essential for drug development. By tailoring the structure of MOFs, researchers have been able to design catalysts with enhanced oxidation capabilities, opening up new possibilities in organic synthesis. MOFs have shown promise in reduction reactions as efficient catalysts for converting various substrates into valuable products (Fig. 12). For instance, MOFs have exhibited high selectivity and activity in converting carbon dioxide into beneficial chemicals, offering a sustainable approach to carbon utilization. Scientists have enhanced these catalysts' reduction performance and stability by optimizing the pore size and metal sites within MOFs.

Furthermore, MOFs have emerged as promising candidates for photocatalysis, harnessing light energy to drive chemical reactions. By incorporating light-absorbing components into their structure, MOFs can facilitate the generation of reactive species that initiate desired transformations [177, 178]. This capability has been leveraged in the degradation of environmental pollutants and the production of solar fuels, highlighting the potential of MOFs in addressing pressing energy and environmental challenges. In electrocatalysis, MOFs have shown great potential for catalyzing electrochemical reactions with high efficiency and

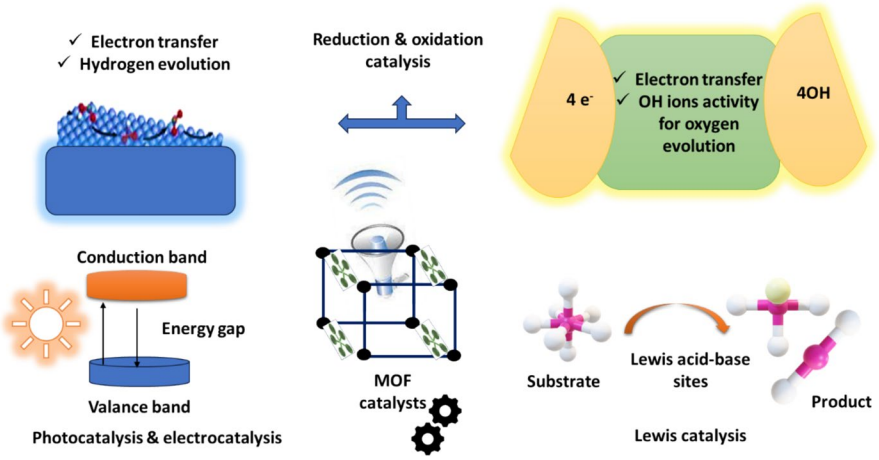

Fig. 12 Schematic representation of MOF properties and high catalytical activities

selectivity. By tuning the electronic properties of MOFs by introducing different metal nodes, researchers have been able to design catalysts for applications such as water splitting, small molecules, and CO_2 reduction [179]. These electrocatalytic MOFs offer a sustainable pathway to clean energy production and storage, contributing to developing renewable energy technologies.

This multifaceted approach enables researchers to design and develop highly effective MFS for various chemical synthesis, energy conversion, and environmental remediation applications. Despite the potential benefits of utilizing MOFs as catalysts, significant challenges must be overcome. These obstacles include instability, a lack of coordination between nodes and linkers, and susceptibility to moisture. These factors can significantly impact the effectiveness of MOF-based catalysts and limit their potential applications in various industries. As such, researchers must continue exploring ways to address these challenges and optimize the use of MOFs in catalytic processes. Through ongoing research and development efforts, it may be possible to unlock the full potential of MOFs as efficient and effective catalysts for a wide range of applications.

Some potential areas for further exploration in using MOFs in catalytic processes include developing new synthesis methods for MOFs with tailored properties, exploring the use of MOFs as support for other catalysts, and investigating the role of defects and surface chemistry in MOF catalysis. Additionally, there is a need to optimize reaction conditions and develop new techniques for characterizing MOF catalysts under realistic operating conditions. By addressing these challenges, it may be possible to unlock the full potential of MOFs as versatile and efficient catalysts for a wide range of chemical transformations.

5 Conclusion

MOF-based catalysts have shown great potential in various catalytic reactions due to their high surface area, tunable pore size, and unique chemical properties. The development of MOF-based catalysts has opened up new opportunities for designing efficient and selective catalysts for various applications. In conclusion, MOF-based catalysts have emerged as a promising class of heterogeneous catalysts with remarkable catalytic performance and stability. Further research is needed to fully understand the underlying mechanisms and optimize the synthesis and design of these materials for specific applications. With continued efforts in this field, MOF-based catalysts are expected to contribute significantly to the advancement of catalysis science and technology. MOF-based catalyst materials have shown great potential in various applications such as gas storage, catalysis, and energy conversion. The unique properties of MOFs, including their high surface area, tunable pore size, and structural diversity, make them attractive for energy-related research. Recent studies have demonstrated the effectiveness of MOFs in areas such as solar cells, fuel cells, and batteries. However, challenges still exist in optimizing the performance and stability of MOF-based catalyst materials. Further research is needed to fully understand their behavior mechanisms and develop new strategies for improving their properties. One promising approach uses post-synthetic modification (PSM) techniques to introduce functional groups into MOFs and enhance their performance. Another strategy involves combining MOFs with other functional components into composite materials to create synergistic effects.

Additionally, advances in computational modeling and simulation can aid in designing and optimizing MOF-based catalyst materials. Overall, MOFs are promising for advancing catalysis-related technologies and addressing global challenges such as climate change and sustainable development. Continued research efforts will be critical in unlocking their full potential for a cleaner and more sustainable future.

Acknowledgements We gratefully acknowledge the Fundação para a Ciência e a Tecnologia (FCT), Portugal, for projects UIDB/00100/2020 (https://doi.org/10.54499/UIDB/00100/2020), UIDP/00100/2020 (https://doi.org/10.54499/UIDP/00100/2020), and LA/P/0056/2020 (https://doi.org/10.54499/LA/P/0056/2020) of Centro de Química Estrutural and Kurukshetra University Kurukshetra-136119, India, for providing a research platform.

Author Contributions Virender: Conceptualization, Data curation, Investigation, Resources, Formal analysis; Vandana Pandey: Conceptualization, Data curation, Investigation, Resources, Formal analysis, Writing-review editing; Gurjaspreet Singh: Supervision, Writing- review editing, Formal analysis; Pankaj Bhatia: Formal analysis; Alexander A. Solovev: Formal analysis; Pawan Kumar Sharma: Investigations, Formal analysis; Brij Mohan: Conceptualization, Supervision, Resources, Formal analysis; Writing-Original draft preparation.

Data Availability No datasets were generated or analysed during the current study.

Declarations

Conflict of interest The authors declare that they have no known competing financial interests or personal relationships that could have appeared to influence the work reported in this paper.

References

1. Chowdhury AH, Salam N, Debnath R, Islam SM, Saha T (2019) Nanomaterials synthesis. Elsevier, Amsterdam, p 265
2. Anglin EJ, Cheng L, Freeman WR, Sailor MJ (2008) Adv Drug Deliv Rev 60:1266
3. Valtchev V, Tosheva L (2013) Chem Rev 113:6734
4. White RJ, Luque R, Budarin VL, Clark JH, Macquarrie DJ (2009) Chem Soc Rev 38:481
5. Liu P, Chen G-F (2014) Porous materials: processing and applications. Elsevier, Amsterdam
6. Gupta S, Tai N-H (2016) J Mater Chem A 4:1550
7. Cai G, Yan P, Zhang L, Zhou H-C, Jiang H-L (2021) Chem Rev 121:12278
8. Inonu Z, Keskin S, Erkey C (2018) ACS Appl Nano Mater 1:5959
9. Wang L, Xu H, Gao J, Yao J, Zhang Q (2019) Coord Chem Rev 398:213016
10. Kumar P, Deep A, Kim K-H (2015) TrAC Trends Anal Chem 73:39
11. Lei J, Qian R, Ling P, Cui L, Ju H (2014) TrAC Trends Anal Chem 58:71
12. Pal TK, De D, Bharadwaj PK (2022) Fuel 320:123904
13. Jiang X, Nie X, Guo X, Song C, Chen JG (2020) Chem Rev 120:7984
14. Horike S, Kitagawa S (2011) Metal-organic frameworks: applications from catalysis to gas storage, vol 1. Wiley, Hoboken
15. Silva P, Vilela SM, Tomé JP, Paz FAA (2015) Chem Soc Rev 44:6774
16. Goetjen TA, Liu J, Wu Y, Sui J, Zhang X, Hupp JT, Farha OK (2020) Chem Commun 56:10409
17. Xu C, Fang R, Luque R, Chen L, Li Y (2019) Coord Chem Rev 388:268
18. Huang W, Zhang W, Yang S, Wang L, Yu G (2023) Small 20:2308019
19. Chen L, Zhang X, Cheng X, Xie Z, Kuang Q, Zheng L (2020) Nanoscale Adv 2:2628
20. Xiao W, Cheng M, Liu Y, Wang J, Zhang G, Wei Z, Li L, Du L, Wang G, Liu H (2023) ACS Catal 13:1759
21. Wang X, Wang Z, Liu Y, Dai H, Zhao Z, Deng J (2024) Top Catal 1-22
22. Mon M, Bruno R, Ferrando-Soria J, Armentano D, Pardo E (2018) J Mater Chem A 6:4912
23. Wang C-Y, Chu H-Y, Wang C-C (2024) Coord Chem Rev 518:216106
24. Nabipour H, Rohani S, Batool S, Yusuff AS (2023) J Environ Chem Eng 11:109131
25. Moosavi SM, Nandy A, Jablonka KM, Ongari D, Janet JP, Boyd PG, Lee Y, Smit B, Kulik HJ (2020) Nat Commun 11:1
26. Moghadam PZ, Chung YG, Snurr RQ (2024) Nat Energy 9:121
27. Xu H, Mguni LL, Yao Y, Hildebrandt D, Jewell LL, Liu X (2024) J Clean Prod 461:142634
28. Zheng K, Tan H, Wang L, Liu J, Ding M, Jia D (2021) Adv Mater Interfaces 8:2002145
29. Zhao R, Liang Z, Zou R, Xu Q (2018) Joule 2:2235
30. Abdelnaby MM, Tayeb IM, Alloush AM, Alyosef HA, Alnoaimi A, Zeama M, Mohammed MG, Onaizi SA (2024) J CO2 Util 79:102647
31. Oschatz M, Antonietti M (2018) Energy Environ Sci 11:57
32. Wang XH, Ling Y, Wu B, Li BL, Li XL, Lei JL, Li NB, Luo HQ (2021) Nano Energy 87:106160
33. Ricco R, Styles MJ, Falcaro P (2019) Metal-organic frameworks (MOFs) for environmental applications. Elsevier, Amsterdam, p 383
34. Yan X, Li P, Song X, Li J, Ren B, Gao S, Cao R (2021) Coord Chem Rev 443:214034
35. Rasheed T (2023) Chemosphere 313:137607
36. Alezi D, Belmabkhout Y, Suyetin M, Bhatt PM, Weseliński ŁJ, Solovyeva V, Adil K, Spanopoulos I, Trikalitis PN, Emwas A-H (2015) J Am Chem Soc 137:13308
37. Mallakpour S, Nikkhoo E, Hussain CM (2022) Coord Chem Rev 451:214262
38. Rojas S, Baati T, Njim L, Manchego L, Neffati F, Abdeljelil N, Saguem S, Serre C, Najjar MF, Zakhama A (2018) J Am Chem Soc 140:9581
39. Chuhadiya S, Suthar D, Patel S, Dhaka M (2021) Coord Chem Rev 446:214115
40. Cao X, Tan C, Sindoro M, Zhang H (2017) Chem Soc Rev 46:2660
41. An M, He M-Q, Lin C, Wu Y, Ai Y, Xin H, Liang Q (2023) Mater Today Nano 22:100330
42. Qin Y, Zhu X, Huang R (2023) Biomater Sci 11:6942
43. Dey S, Mehta N (2020) Resour Environ Sustain 2:100006
44. Bavykina A, Kolobov N, Khan IS, Bau JA, Ramirez A, Gascon J (2020) Chem Rev 120:8468
45. Wei Y-S, Zhang M, Zou R, Xu Q (2020) Chem Rev 120:12089
46. Chen J, Shen K, Li Y (2017) ChemSusChem 10:3165

47. Hou X, Sun J, Lian M, Peng Y, Jiang D, Xu M, Li B, Xu Q (2023) Macromol Mater Eng 308:2200469
48. Alhumaimess MS (2020) J Saudi Chem Soc 24:461
49. Remya V, Kurian M (2019) Int Nano Lett 9:17
50. Qin Y, Li Z, Duan Y, Guo J, Zhao M, Tang Z (2022) Matter 5:3260
51. Gao F, Yan R, Shu Y, Cao Q, Zhang L (2022) RSC Adv 12:10114
52. Shen K, Chen X, Chen J, Li Y (2016) ACS Catal 6:5887
53. Li R, Chen T, Pan X (2021) ACS Nano 15:3808
54. Begum S, Hassan Z, Brase S, Tsotsalas M (2020) Langmuir 36:10657
55. Healy C, Patil KM, Wilson BH, Hermanspahn L, Harvey-Reid NC, Howard BI, Kleinjan C, Kolien J, Payet F, Telfer SG (2020) Coord Chem Rev 419:213388
56. Goel N, Mishra S, Kumar N (2023) Advanced functional metal-organic frameworks. CRC Press, Boca Raton, p 17
57. Al Amery N, Abid HR, Al-Saadi S, Wang S, Liu S (2020) Mater Today Chem 17:100343
58. Khan MS, Shahid M (2022) Electrochemical applications of metal-organic frameworks. Elsevier, Amsterdam, p 17
59. Geng S, Lin E, Li X, Liu W, Wang T, Wang Z, Sensharma D, Darwish S, Andaloussi YH, Pham T (2021) J Am Chem Soc 143:8654
60. Klinowski J, Paz FAA, Silva P, Rocha J (2011) Dalton Trans 40:321
61. Yamashita K, Kashiwagi K, Agrawal A, Daiguji H (2017) Mol Phys 115:328
62. Usman J, Esham MIM, Yogarathinam LT, Abba SI, El-Badawy T, Othman MHD, Aljundi IH (2024) Advanced ceramics for photocatalytic membranes. Elsevier, Amsterdam, p 179
63. Muslim M, Ali A, Ahmad M (2024) Synthesis of metal-organic frameworks via water-based routes. Elsevier, Amsterdam, p 73
64. Azizi SMM, Haffiez N, Mostafa A, Hussain A, Abdallah M, Al-Mamun A, Bhatnagar A, Dhar BR (2024) Renew Sustain Energy Rev 200:114453
65. Wang J, Wei Y, Ma Z (2020) Appl Sci 10:1311
66. Rosen AS, Fung V, Huck P, O'Donnell CT, Horton MK, Truhlar DG, Persson KA, Notestein JM, Snurr RQ (2022) npj Comput Mater 8:1
67. Mohamed SA, Zhao D, Jiang J (2023) Commun Mater 4:79
68. Kalaj M, Bentz KC, Ayala S Jr, Palomba JM, Barcus KS, Katayama Y, Cohen SM (2020) Chem Rev 120:8267
69. Chen L, Luque R, Li Y (2017) Chem Soc Rev 46:4614
70. Rosseinsky M (2004) Microporous Mesoporous Mater 73:15
71. Hwang J, Ejsmont A, Freund R, Goscianska J, Schmidt BV, Wuttke S (2020) Chem Soc Rev 49:3348
72. Łuczak J, Kroczewska M, Baluk M, Sowik J, Mazierski P, Zaleska-Medynska A (2023) Adv Colloid Interface Sci 314:102864
73. Li D, Xu H-Q, Jiao L, Jiang H-L (2019) EnergyChem 1:100005
74. Du Y, Jia X, Zhong L, Jiao Y, Zhang Z, Wang Z, Feng Y, Bilal M, Cui J, Jia S (2022) Coord Chem Rev 454:214327
75. Ahmed I, Mondol MMH, Jung MJ, Lee GH, Jhung SH (2023) Coord Chem Rev 475:214912
76. Liu JL, Ma YC, Yang T, Hu R, Yang YH (2021) Microchim Acta 188:1
77. Lu S, Xiao Y, Zhao Q, Zhao W, He G (2023) Sep Purif Technol 306:122665
78. Yadav A, Kanoo P (2019) Chem Asian J 14:3531
79. Vermoortele F, Ameloot R, Vimont A, Serre C, De Vos D (2011) Chem Commun 47:1521
80. Srirambalaji R, Hong S, Natarajan R, Yoon M, Hota R, Kim Y, Ko YH, Kim K (2012) Chem Commun 48:11650
81. Toyao T, Fujiwaki M, Horiuchi Y, Matsuoka M (2013) RSC Adv 3:21582
82. Rafiee Z (2021) J Iran Chem Soc 18:2657
83. Tu B, Pang Q, Xu H, Li X, Wang Y, Ma Z, Weng L, Li Q (2017) J Am Chem Soc 139:7998
84. Nagaraj A, Amarajothi D (2017) J Colloid Interface Sci 494:282
85. Dhakshinamoorthy A, Asiri AM, Concepcion P, Garcia H (2017) Chem Commun 53:9998
86. Nikseresht A, Ghasemi S, Parak S (2018) Polyhedron 151:112
87. Han L, Qi H, Zhang D, Ye G, Zhou W, Hou C, Xu W, Sun Y (2017) New J Chem 41:13504
88. Wang H, Rassu P, Wang X, Li H, Wang X, Wang X, Feng X, Yin A, Li P, Jin X (2018) Angew Chem Int Ed 57:16416
89. Huang S, Yang K-L, Liu X-F, Pan H, Zhang H, Yang S (2017) RSC Adv 7:5621

90. Li X-Y, Ma L-N, Liu Y, Hou L, Wang Y-Y, Zhu Z (2018) ACS Appl Mater Interfaces 10:10965
91. Gulati S, Vijayan S, Kumar S, Harikumar B, Trivedi M, Varma RS (2023) Coord Chem Rev 474:214853
92. Agarwal RA, Gupta AK, De D (2019) Cryst Growth Des 19:2010
93. Lyu J, Zhang X, Li P, Wang X, Buru CT, Bai P, Guo X, Farha OK (2019) Chem Mater 31:4166
94. Jamil U, Khoja AH, Liaquat R, Naqvi SR, Omar WNNW, Amin NAS (2020) Energy Convers Manag 215:112934
95. Gupta AK, Guha N, Krishnan S, Mathur P, Rai DK (2020) J CO2 Util 39:101173
96. Xu Y-P, Wang Z-Q, Tan H-Z, Jing K-Q, Xu Z-N, Guo G-C (2020) Catal Sci Technol 10:1699
97. Feng X, Song Y, Lin W (2021) J Am Chem Soc 143:8184
98. Liu Y, Zhao P, Duan C, He C (2021) RSC Adv 11:34779
99. Ronaghi N, Shade D, Moon HJ, Najmi S, Cleveland JW, Walton KS, France S, Jones CW (2021) ACS Sustain Chem Eng 9:11581
100. Gandhi S, Sharma V, Koul IS, Mandal SK (2023) Catal Lett 153:887
101. Tian XR, Jiang XL, Hou SL, Jiao ZH, Han J, Zhao B (2022) Angew Chem 134:e202200123
102. Peralta RA, Lyu P, López-Olvera A, Obeso JL, Leyva C, Jeong NC, Ibarra IA, Maurin G (2022) Angew Chem 134:e202210857
103. Hou L, Chen X, Zhang X, Tang Y, Yao Y, Lin T, Zhao S (2023) Sens Actuators B Chem 375:132902
104. Lan M-Y, Li Y-H, Wang C-C, Li X-J, Cao J, Meng L, Gao S, Ma Y, Ji H, Xing M (2024) Nat Commun 15:7208
105. Zhao Q, Wang C-C, Wang P (2022) Chin Chem Lett 33:4828
106. Li Y-H, Wang C-C, Wang F, Liu W, Chen L, Zhao C, Fu H, Wang P, Duan X (2023) Appl Catal B 331:122699
107. Wang F-X, Wang C-C, Du X, Li Y, Wang F, Wang P (2022) Chem Eng J 429:132495
108. Fu H, Song X-X, Wu L, Zhao C, Wang P, Wang C-C (2020) Mater Res Bull 125:110806
109. Ji S, Chen Y, Fu Q, Chen Y, Dong J, Chen W, Li Z, Wang Y, Gu L, He W (2017) J Am Chem Soc 139:9795
110. Kim S, Lee J, Jeoung S, Moon HR, Kim M (2020) Chem Eur J 26:7568
111. Yang S, Qiu X, Jin P, Dzakpasu M, Wang XC, Zhang Q, Yang L, Ding D, Wang W, Wu K (2018) Chem Eng J 353:329
112. Baek J, Rungtaweevoranit B, Pei X, Park M, Fakra SC, Liu Y-S, Matheu R, Alshmimri SA, Alshehri S, Trickett CA (2018) J Am Chem Soc 140:18208
113. Bhadra BN, Jhung SH (2019) Appl Catal B 259:118021
114. Wang X, Ying J, Mai Y, Zhang J, Chen J, Wen M, Yu L (2019) Catal Sci Technol 9:5845
115. Guo Z, Song L, Xu T, Gao D, Li C, Hu X, Chen G (2019) Mater Chem Phys 226:338
116. Li J-R, Wang F-K, He C, Huang C, Xiao H (2020) Powder Technol 363:95
117. Lyu P, Maurin G (2020) ACS Catal 10:9445
118. Zhang S, Li JPH, Zhao J, Wu D, Yuan B, Hernández WY, Zhou W-J, He T, Yu Y, Yang Y (2021) Nano Res 14:479
119. Ma Y, Wang L, Ma J, Wang H, Zhang C, Deng H, He H (2021) ACS Catal 11:6614
120. Zhang Q, Luo Q, Wu Y, Yu R, Cheng J, Zhang Y (2021) RSC Adv 11:33416
121. Wang L, Sun Y, Zhu Y, Zhang J, Ding J, Gao J, Ji W, Li Y, Wang L, Ma Y (2022) J Colloid Interface Sci 622:577
122. Hao J, Jiang Z, Khan HA, El Tall O, Farooq A (2022) Fuel 318:123638
123. Zhou T, Wang S, Zhang C, Yao Y, Chen Y, Lu S, Liao X (2023) Fuel 339:127396
124. Mohtasham H, Rostami M, Gholipour B, Sorouri AM, Ehrlich H, Ganjali MR, Rostamnia S, Rahimi-Nasrabadi M, Salimi A, Luque R (2023) Chemosphere 310:136625
125. Moghadaskhou F, Tadjarodi A, Mollahosseini A, Maleki A (2023) ACS Appl Mater Interfaces 15:4021
126. Miyah Y, El Messaoudi N, Benjelloun M, Georgin J, Franco DSP, Acikbas Y, Kusuma HS, Sillanpää M (2024) Mater Today Sustain 28:100985
127. Manzoor MH, Naz N, Naqvi SMG, Ashraf S, Ashiq MZ, Verpoort F (2024) Appl Mater Today 40:102358
128. Jin H-G, Zhao P-C, Qian Y, Xiao J-D, Chao Z-S, Jiang H-L (2024) Chem Soc Rev 53:9378
129. Guo D, Chen L, Li Y (2024) Catalysis in confined frameworks: synthesis, characterization, and applications. Wiley, Hoboken, p 219
130. Yusran Y, Xu D, Fang Q, Zhang D, Qiu S (2017) Microporous Mesoporous Mater 241:346

131. Zhang W, Shi W, Ji W, Wu H, Gu Z, Wang P, Li X, Qin P, Zhang J, Fan Y (2020) ACS Catal 10:5805
132. Wang X, Zhang X, Pandharkar R, Lyu J, Ray D, Yang Y, Kato S, Liu J, Wasson MC, Islamoglu T (2020) ACS Catal 10:8995
133. Dai Y, Li X, Wang L, Xu X (2021) New J Chem 45:22908
134. Yan X, Chen L, Song H, Gao Z, Wei H, Ren W, Wang W (2021) New J Chem 45:18268
135. Zhao M, Yuan K, Wang Y, Li G, Guo J, Gu L, Hu W, Zhao H, Tang Z (2016) Nature 539:76
136. Li J, Xia W, Tang J, Gao Y, Jiang C, Jia Y, Chen T, Hou Z, Qi R, Jiang D (2022) J Am Chem Soc 144:9280
137. Dharman RK, Francis BM, Ponraj JS, Muthuvijayan S, Manavalan RK, Harisingh S, Balasubramanian S, Dhanabalan SC (2022) J Mater Res Technol 17:1760
138. Song Z, Li R, Wen D, Pei J, Zhu H, Ruan S (2023) ACS Mater Lett 5:473
139. Nagajyothi P, Ramaraghavulu R, Pavani K, Shim J (2023) Mater Lett 336:133837
140. Gao P, Sun X-Y, Liu B, Lian H-T, Liu X-Q, Shen J-S (2018) J Mater Chem C 6:8105
141. Sun K, Qian Y, Jiang HL (2023) Angew Chem Int Ed 62:e202217565
142. Wang C-C, Li J-R, Lv X-L, Zhang Y-Q, Guo G (2014) Energy Environ Sci 7:2831
143. Behera P, Subudhi S, Tripathy SP, Parida K (2022) Coord Chem Rev 456:214392
144. Reddy CV, Reddy KR, Harish V, Shim J, Shankar M, Shetti NP, Aminabhavi TM (2020) Int J Hydrogen Energy 45:7656
145. Guo J, Wan Y, Zhu Y, Zhao M, Tang Z (2021) Nano Res 14:2037
146. Siddig LA, Alzard RH, Nguyen HL, Göb CR, Alnaqbi MA, Alzamly A (2022) ACS Omega 7:9958
147. Shang S, Xiong W, Yang C, Johannessen B, Liu R, Hsu H-Y, Gu Q, Leung MK, Shang J (2021) ACS Nano 15:9670
148. Qin J, Pei Y, Zheng Y, Ye D, Hu Y (2023) Appl Catal B 325:122346
149. Li Y-H, Liu M-Y, Wei Y-W, Wang C-C, Wang P (2023) Environ Sci Nano 10:672
150. Song Y, Li Z, Zhu Y, Feng X, Chen JS, Kaufmann M, Wang C, Lin W (2019) J Am Chem Soc 141:12219
151. Wen M, Mori K, Kuwahara Y, An T, Yamashita H (2017) Appl Catal B 218:555
152. Chen Y, Ji S, Sun W, Lei Y, Wang Q, Li A, Chen W, Zhou G, Zhang Z, Wang Y (2020) Angew Chem 132:1311
153. Zeng L, Wang Z, Wang Y, Wang J, Guo Y, Hu H, He X, Wang C, Lin W (2019) J Am Chem Soc 142:75
154. Huang W, Jing C, Zhang X, Tang M, Tang L, Wu M, Liu N (2018) Chem Eng J 349:603
155. Du X-D, Yi X-H, Wang P, Zheng W, Deng J, Wang C-C (2019) Chem Eng J 356:393
156. Zhao Q, Yi X-H, Wang C-C, Wang P, Zheng W (2022) Chem Eng J 429:132497
157. Mukherjee D, Van der Bruggen B, Mandal B (2022) Chemosphere 295:133835
158. Habila M, Alhenaki B, El-Marghany A, Sheikh M, Ghfar A, ALOthman Z, Soylak M (2020) J Sep Sci 43:3103
159. Yilmaz E, Tut Y, Turkoglu O, Soylak M (2018) J Iran Chem Soc 15:1721
160. Deshmukh K, Pandey M (2024) Nanostructured Materials for Energy Storage, 4 Volumes. John Wiley & Sons
161. Qiu T, Liang Z, Guo W, Tabassum H, Gao S, Zou R (2020) ACS Energy Lett 5:520
162. Li P, Jin Z, Qian Y, Fang Z, Xiao D, Yu G (2019) ACS Energy Lett 4:1793
163. Wang Q, Astruc D (2019) Chem Rev 120:1438
164. Liao P-Q, Shen J-Q, Zhang J-P (2018) Coord Chem Rev 373:22
165. Ye Z, Jiang Y, Li L, Wu F, Chen R (2023) eScience 3:100107
166. Li J, Huang W, Wang M, Xi S, Meng J, Zhao K, Jin J, Xu W, Wang Z, Liu X (2018) ACS Energy Lett 4:285
167. Li D, Qin Y, Liu J, Zhao H, Sun Z, Chen G, Wu DY, Su Y, Ding S, Xiao C (2022) Adv Funct Mater 32:2107056
168. Zhai Q, Hu K-J, Shi Y, Ji H, Wu H, Ren Y, Wang B, Tang S, Ma Y, Cui M (2023) J Phys Chem Lett 14:1156
169. Xu Y, Yang C, Deng Q, Zhou Y, Mao C, Song Y, Zhu M, Zhang Y (2023) Appl Surf Sci 612:155870
170. Patel KB, Parmar B, Ravi K, Patidar R, Chaudhari JC, Srivastava DN, Bhadu GR (2023) Appl Surf Sci 616:156499
171. Vijayakumar E, Ramakrishnan S, Sathiskumar C, Yoo DJ, Balamurugan J, Noh HS, Kwon D, Kim YH, Lee H (2022) Chem Eng J 428:131115

172. Hwang S-M, Choi SY, Youn MH, Lee W, Park KT, Gothandapani K, Grace AN, Jeong SK (2020) ACS Omega 5:23919
173. Zhong H, Ghorbani-Asl M, Ly KH, Zhang J, Ge J, Wang M, Liao Z, Makarov D, Zschech E, Brunner E (2020) Nat Commun 11:1409
174. Liu J, Zhu D, Guo C, Vasileff A, Qiao SZ (2017) Adv Energy Mater 7:1700518
175. Zhang Y, Qi L (2022) Nanoscale 14:12196
176. Chakraborty D, Yurdusen A, Mouchaham G, Nouar F, Serre C (2023) Adv Funct Mater 34:2309089
177. Mohamadpour F, Amani AM (2024) RSC Adv 14:20609
178. Morshedy AS, El-Fawal EM, Zaki T, El-Zahhar AA, Alghamdi MM, El Naggar AM (2024) Inorg Chem Commun 163:112307
179. Sun K, Huang Y, Sun F, Wang Q, Zhou Y, Wang J, Zhang Q, Zheng X, Fan F, Luo Y (2024) Nat Chem 16:1638
180. Chu L, Guo J, Huang Z, Yang H, Yang M, Wang G (2023) Fuel 332:126012

Authors and Affiliations

Virender Virender[1] · Vandana Pandey[2] · Gurjaspreet Singh[3] · Pawan Kumar Sharma[4] · Pankaj Bhatia[2] · Alexander A. Solovev[5] · Brij Mohan[6]

✉ Vandana Pandey
vandanap.chem@kuk.ac.in

✉ Brij Mohan
brij.mohan@tecnico.ulisboa.pt

Virender Virender
chem2022virenderphd@kuk.ac.in

[1] Department of Chemistry, Deenbandhu Chhotu Ram University of Science and Technology, Murthal, Sonepat 131039, Haryana, India

[2] Department of Chemistry, Kurukshetra University Kurukshetra, Kurukshetra 136119, India

[3] Department of Chemistry and Centre of Advanced Studies, Panjab University, Chandigarh 160014, India

[4] Department of Chemistry, School of Basic Sciences, Central University of Haryana, Mahendragarh 123031, Haryana, India

[5] Department of Materials Science and State Key Laboratory of Molecular Engineering of Polymers, Fudan University, Shanghai 200433, People's Republic of China

[6] Centro de Química Estrutural, Institute of Molecular Sciences, Instituto Superior Técnico, Universidade de Lisboa, Av. Rovisco Pais, 1049-001 Lisbon, Portugal